

# Magnetic susceptibility of a $\text{CuO}_2$ plane in the $\text{La}_2\text{CuO}_4$ system : I. RPA treatment of the Dzyaloshinskii-Moriya Interactions

K. V. Tabunshchuk

Department of Physics, Queen's University, Kingston ON K7L 3N6 Canada and  
Institute for Condensed Matter Physics, Lviv, Ukraine

R. J. Gooding

Department of Physics, Queen's University, Kingston ON K7L 3N6 Canada  
(dated: March 23, 2022)

Motivated by recent experiments on undoped  $\text{La}_2\text{CuO}_4$ , which found pronounced temperature-dependent anisotropies in the low-field magnetic susceptibility, we have investigated a two-dimensional square lattice of  $S = 1/2$  spins that interact via Heisenberg exchange plus the symmetric and anti-symmetric Dzyaloshinskii-Moriya anisotropies. We describe the transition to a state with long-ranged order, and find the spin-wave excitations, with a mean-field theory, linear spin-wave analysis, and using Tyablikov's RPA decoupling scheme. We find the different components of the susceptibility within all of these approximations, both below and above the Neel temperature, and obtain evidence of strong quantum fluctuations and spin-wave interactions in a broad temperature region near the transition.

## I. INTRODUCTION

Quantum magnetism of low-dimensional systems has attracted considerable attention in recent years, in part due to the strong interest in the cuprate superconductors. For example, it has been postulated that a strong antiferromagnetic (AF) exchange interaction may be responsible for the high-temperature superconductivity in these compounds.<sup>1</sup>

The ubiquitous structural and electronic constituent of this latter class of materials is the  $\text{CuO}_2$  plane, and in this paper we consider the magnetic properties of such planes in their undoped state. In particular, we consider the temperature dependence of the static, uniform magnetic susceptibility for a single plane in an undoped  $\text{La}_2\text{CuO}_4$  crystal. This system is known to be an AF insulator with a very simple structure, namely it can be approximately thought of as one  $\text{CuO}_2$  plane stacked between  $\text{LaO}$  planes, with this structural unit repeated, in a body-centred tetragonal pattern, throughout all space. However, a small orthorhombic distortion introduces important spin-orbit couplings into the magnetic Hamiltonian, leading to an AF state with a weak canted ferromagnetic moment. These spin-orbit interactions are central to the results presented in this paper.

As is known from the start of research on the cuprate superconductors, a complete knowledge of the properties of the spin- $\frac{1}{2}$  quantum Heisenberg AF on a square lattice is an absolute necessity.<sup>2</sup> However, some experiments have demonstrated that a complete description of the magnetic behaviour found in, e.g.  $\text{La}_2\text{CuO}_4$ , requires additional physics. Examples include (i) weak ferromagnetism in the low-temperature orthorhombic (LTO) phase,<sup>3,4</sup> (ii) spin wave gaps with in- and out-of-plane modes,<sup>5</sup> and perhaps most importantly, (iii) the unusual anisotropy of the magnetic susceptibility observed by Lavrov, Ando, Komiyama and Tsukada.<sup>6</sup> It was this latter

experiment that led us to complete a sequence of theoretical investigations on a model that should describe such a three-dimensional array of such  $\text{CuO}_2$  planes modelling  $\text{La}_2\text{CuO}_4$ , a structure similar to those found in many cuprate superconductors. This manuscript summarizes the first of these studies, that concerned with a single  $\text{CuO}_2$  plane, with this plane described by a near-neighbour Heisenberg model plus spin-orbit couplings as embodied by the antisymmetric and symmetric Dzyaloshinskii-Moriya (DM) interactions.<sup>7,8</sup>

An important point needs to be raised to clarify the applicability of this work to a real physical system, such as  $\text{La}_2\text{CuO}_4$ . Firstly, note that according to the Mermin-Wagner theorem a two-dimensional (2D) system with a continuous symmetry cannot undergo a continuous phase transition, at any nonzero temperature, to a state with true long-ranged order. However, when one includes both the antisymmetric and symmetric DM interactions this symmetry is lifted, and thus the model that we study in this paper will have a true phase transition to an ordered phase at some nonzero temperature, which we shall label by  $T_N$ , in analogy to the Neel ordering temperature of a pure antiferromagnet. So, the ordered phase for our model of a single plane will include a weak ferromagnetic canted moment, as well as long-ranged AF order. Note that current estimates<sup>9</sup> of another interaction present in the physical  $\text{La}_2\text{CuO}_4$  system, that being a very weak AF interlayer coupling which is usually denoted by  $J_z$ , is that this energy scale is close to that of the DM interactions, and thus it is likely that both this exchange and the DM interactions are roughly equally responsible for the observed transition. This serves to emphasize that our study of a single plane is not expected to accurately explain all of the observed magnetic properties of  $\text{La}_2\text{CuO}_4$ ; in fact, this work stands alone as a theoretical study of an isolated plane, but it is of considerable interest to learn which experimental data can and which data can not be explained by such a single-plane model.

We focus on the role of the DM interaction between the neighbouring spins in a  $\text{CuO}_2$  plane. This interaction arises from the orthorhombic distortion in  $\text{La}_2\text{CuO}_4$  (which is associated with the small tilt of the  $\text{CuO}_6$  octahedra) together with the spin-orbit interaction. The DM interaction leads to a small canting of the Cu spins out of the plane, so that the weak ferromagnetic order appears in each  $\text{CuO}_2$  plane, and subsequently allows for the formation of 3D AF order. This allows one to observe a pronounced peak in zero-field magnetic susceptibility,  $\chi^0(T)$ , and the earliest work on the importance of this interaction focused on DM physics. To be specific, Thio et al.<sup>3,11</sup> analyzed their susceptibility data using a Landau theory expanded to sixth order, for a 2D Heisenberg antiferromagnet with interlayer coupling and the DM-generated terms. They obtained reasonable fits of their theory to the susceptibility and field-dependent magnetization data, and deduced parameters which characterized magnetic properties of the  $\text{La}_2\text{CuO}_4$  system. As we shall explain below, we believe that the necessity of incorporating such higher-order terms into their fits is suggestive of the important role played by spin-wave interactions, a conclusion consistent with the results presented in this, and our future manuscripts on this problem.

Investigations of the magnetic ground state of  $\text{La}_2\text{CuO}_4$  were performed by several groups of authors, usually within the framework of the linear spin-wave (SW) theory. The calculations were based on an effective model Hamiltonian derived by Moriya's perturbation theory<sup>8</sup> applied to Hubbard type Hamiltonians by taking into account the spin-orbit coupling. In the most general form, the effective spin Hamiltonian, in addition to the isotropic exchange interaction, includes the above-mentioned antisymmetric and symmetric DM interactions. The first microscopic derivation of the spin Hamiltonian was performed by Coey, Rice, and Zhang;<sup>12</sup> they estimated the antisymmetric DM coupling constants and showed that when the DM vectors alternate a net ferromagnetic moment may be generated in the ground state. Shekhtman, Entin-Wohlman, and Aharony<sup>13</sup> subsequently showed that the symmetric anisotropies contribute to the magnetic energy in the same order as the antisymmetric DM anisotropy, and can never be neglected. Several groups<sup>9,14,15</sup> reexamined the Moriya's theory and found expressions for the effective spin Hamiltonian which includes both types of anisotropies. The linear SW theory applied to such models at  $T = 0$  allows one to obtain previously reported values of the spin-wave gaps at the centre of the 2D Brillouin zone, as well as to estimate the magnitudes of the anisotropic-exchange interactions. However, a detailed consideration of the model with the antisymmetric and symmetric DM anisotropies at nonzero temperatures is up to now absent from the literature.

A very rough and simple approximation which can be used to study the effective magnetic model at finite temperatures is the mean-field approximation (MFA). The

MFA ignores effects of fluctuations and correlations between the spins, hence, it fails for  $T$  near  $T_N$  and gives no short-range order above the transition temperature. At very low  $T$  the noninteracting SW theory is useful, and it gives a successful prediction of the energy of low-lying excited states, and correctly reproduces the dominant term in the low- $T$  magnetization. But, it fails near the phase transition point. To analyze the high temperature behaviour the  $1/T$  expansion method can be employed. But, since the  $\text{La}_2\text{CuO}_4$  crystal ordering temperature is much smaller than the magnitude of the superexchange interaction ( $T_N \ll J$ ), the high-temperature expansion (to the first few orders in  $J/T$ ) is not able to discuss the temperature region of interest, that is  $T$  near the transition temperature.

In the present paper time we consider the 2D spin- $\frac{1}{2}$  anisotropic quantum Heisenberg antiferromagnet over the entire temperature range including both the symmetric and anti-symmetric DM interactions. We employ the technique of double-time temperature-dependent Green's functions within the framework of the random-phase approximation (RPA). The first time such a scheme was used was by Tyablikov,<sup>16</sup> and he applied this formalism to the Heisenberg ferromagnet (the RPA for magnetic models is often referred to as Tyablikov's decoupling approximation). This work was generalized by Liu<sup>17</sup> to obtain the longitudinal correlation function, and this latter study is important in the development presented in our paper. The important feature of this technique is that it deals with the entire temperature region and is in a good agreement with the SW theory at low- $T$ , as well as with  $1/T$  expansions at high- $T$ . In this paper, within such a scheme, we find the transition temperature at which long-range order would be established for an isolated plane. We obtain the excitation spectrum, sublattice magnetization and susceptibility tensor as function of temperature and coupling constants. We also employ the MFA and SW theories to compare results of all of these approximation schemes, and note the essential differences between them.

Of course, many investigations of the 2D spin- $\frac{1}{2}$  have been completed previous to this work. We have already mentioned the most popular and simple methods to study spin models, that is phenomenological Landau theory, linear SW theory, the MFA, and high-temperature expansions. They yield an analytical description of a wide range of physical properties and are very useful for practical purposes. At the same time the great progress in the understanding of the ground state, thermodynamic properties, and spin dynamics of the Heisenberg magnets was made with the use of the newer and more complicated analytical schemes. Arovas and Auerbach<sup>18</sup> used a path-integral formulation of the MFA theory within the Schwinger-boson representation. This method corresponds to the large- $N$  limit of the generalized  $\text{SU}(N)$  model; however, various difficulties with this method have been discussed in the literature.<sup>19,20</sup> Takahashi<sup>21</sup> has formulated and successfully applied the so-called

modified SW theory to the Heisenberg model which reproduced the results of conventional SW theory and is closely related to the Schwinger-boson theory. For the one dimensional chain, Takahashi's modified SW theory yields very good agreement with Bethe ansatz results, as well as for the 2D classical ferromagnet at low-T (in that it agrees with Monte Carlo results). A self-consistent SW theory that is based on the boson-pseudofermion representation, was developed to study thermodynamics of 2D systems, and was also applied to S=1 systems with an Ising-anisotropy 2D magnets.<sup>22</sup> An important feature of all these methods is that they can be used to describe both the ordered and disordered (i.e. the case of no long-range order) states.

Other related work includes: (i) The fermion representation to perform a  $1/N$  expansion was used by Alick and Marston,<sup>23</sup> large-S 2D Heisenberg antiferromagnet in the long-wavelength limit; and (ii) based on the diagrammatic method for the spin operators, the thermodynamics and the longitudinal spin dynamics of Heisenberg magnets were studied.<sup>24,25</sup> However, the most noteworthy success in the investigation of this system is the work of Chakravarty et al.<sup>26</sup>, who used a renormalization-group approach to the quantum nonlinear model, the latter of which describes the low-T behaviour of the 2d Heisenberg AF in the long-wavelength limit.

As will become apparent below, the formalism that we have chosen to implement is more appropriate for this problem than any of those listed above, or the theories listed above are too complicated to invoke when one goes beyond the 2D spin- $\frac{1}{2}$  Heisenberg AF and includes spin-orbit couplings.

The above few paragraphs summarize theoretical efforts that were directed towards the understanding of the 2D S=1/2 square lattice AF. The application of these and related work to describe the magnetic properties of so-called single-layer cuprate superconductors, such as  $\text{La}_2\text{CuO}_4$ , has attracted the attention of many theorists, and fortunately an extensive review of this work, written by Johnston, already exists.<sup>27</sup> In this review<sup>27</sup> one can

find the comparison of the temperature dependence of the magnetic susceptibility for an AF Heisenberg square lattice calculated by different analytical methods and quantum Monte Carlo calculations, and, apart from the (post-review) data given by Lavrov et. al.<sup>6</sup>, the application of the analytical predictions together with the numerical results show very good fitting to the experimental data for the different single-layer cuprate compounds.

Our paper is organized as follows. In xII we present the model Hamiltonian that we will study, introduce a convenient coordinate transformation with which it is simple to complete analytical calculations, and then derive the transformation that relates the static uniform susceptibility in both coordinate systems. In xIII we derive and describe the MFA results, and then in xIV we present our derivations from applying the Tyablikov/Liu approach to our model Hamiltonian. In xV we present a detailed ex-

amination of numerical results that follow from our work, including a comparison of MFA, RPA and SW theories. Finally, in xVI we summarize our paper including a brief discussion of the remainder of the work that we have completed on the full three-dimensional problem.

## II. MODEL AND DEFINITIONS:

### A. Model Hamiltonian and the initial representation

We consider a model for the Cu spins that are present in the  $\text{CuO}_2$  planes of a  $\text{La}_2\text{CuO}_4$  crystal in the low-temperature orthorhombic (LTO) phase and employ a square lattice with nearest-neighbour interactions described by the following effective magnetic Hamiltonian:<sup>13,14</sup>

$$H = J \sum_{\langle ij \rangle} \mathbf{S}_i \cdot \mathbf{S}_j + \sum_{\langle ij \rangle} D_{ij} (S_i^x S_j^x - S_i^y S_j^y) + \sum_{\langle ij \rangle} S_i^z S_j^z \quad (1)$$

This Hamiltonian consists of the superexchange interaction together with the antisymmetric Dzyaloshinskii-Moriya (DM) interaction (D term) and the symmetric pseudodipolar interaction ( $\hat{D}$  term). As was discussed in the introduction, the DM and pseudodipolar anisotropies arise as a result of the mixture of Hubbard-type interaction energies and spin-orbit coupling in the low symmetry crystal structure.

For the LTO phase, we use anisotropic interactions given by of the following form

$$D_{ab} = \frac{d}{2} (1; 1; 0); \quad D_{ac} = \frac{d}{2} (1; -1; 0); \quad (2)$$

and

$$\hat{D}_{ab} = \begin{pmatrix} 0 & 1 & 0 \\ 1 & 2 & 0 \\ 0 & 0 & 3 \end{pmatrix} A; \quad \hat{D}_{ac} = \begin{pmatrix} 0 & 1 & 0 \\ 1 & 2 & 0 \\ 0 & 0 & 3 \end{pmatrix} A; \quad (3)$$

where the corresponding coordinates, in what we refer to as the "initial representation" in the LTO phase, are shown in Fig. 1(a). Note that the DM vector given in Eq. (2) alternates in sign on successive bonds in the  $a$   $b$  and in the  $a$   $c$  direction of the lattice, as is represented schematically by the double arrows in Fig. 1(b).

We mention that the symmetric tensor  $\hat{D}$  has been obtained by several authors<sup>9,13,14,15,28</sup> in different forms. We have chosen the general form of this tensor, from which other specialized choices can be extracted. For instance, the form of the symmetric tensor obtained by Koshibae, Ohta, and Makiawa<sup>14</sup> can be recovered from this definition if  $\hat{D}_{33} = \hat{D}_{22} = 1$ .

In the LTO phase the classical ground state is determined uniquely,<sup>14,15</sup> and below the Neel temperature the Cu spin structure shows long-range antiferromagnetic order with weak ferromagnetism (viz. all spins cant out of

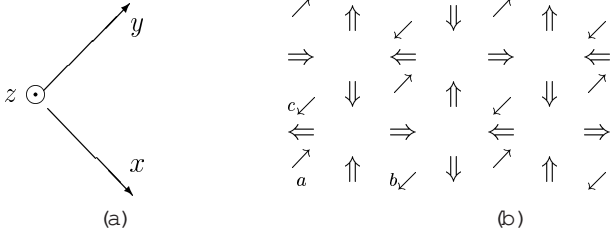


FIG. 1: (a) Coordinates in the initial representation. (b) Thin arrows  $\parallel$  the Cu spins, open arrows  $\parallel$  the DM vectors.

the plane). To be concrete, in the classical ground state the spins are canted from in-plane antiferromagnetic order by a small angle given by

$$= \frac{1}{2} \tan^{-1} \frac{p/2}{J + \frac{1}{2}(1 + \beta)}; \quad (4)$$

and each plane has a net ferromagnetic moment in the  $z$  direction perpendicular to the  $\text{CuO}_2$  planes (weak ferromagnetism).

In the simplified case of the zero pseudodipolar interaction ( $\beta = 0$ ) it was found<sup>12,29</sup> that the ground-state spin configuration exhibits the rotational symmetry about the DM vector which is the origin of the Goldstone mode in the spin-wave spectrum. Since in this simplified case there is a continuous symmetry in the ground state, the thermal fluctuations destroy the long-range order for any  $T > 0$ , according to the Mermin and Wagner theorem.<sup>30</sup> In the general case of the model Hamiltonian of Eq. (1), the continuous symmetry no longer exists and the spin-

wave spectrum is gapped in the long wavelength limit  $q = 0$ . Consequently, the effect of fluctuations is reduced. That is, the DM ( $D \neq 0$ ) together with pseudodipolar ( $\beta \neq 0$ ) interactions can give rise to long-range order for low (but nonzero) temperatures even for the purely two-dimensional case ( $T_N > 0$ ), and the Mermin and Wagner theorem does not preclude the possibility of a nonzero sublattice magnetization for nonzero temperatures in this general case. (Note that this does not imply that the transition to 3d long-ranged magnetic order is not influenced by the inter-planar exchange coupling, but simply that this latter coupling is not, in general, necessary to achieve such order.)

## B. Characteristic representation

In solving this system, it is more convenient (theoretically) to transform from the initial representation, given above, to the characteristic representation (CR) in which the quantization axis ( $z$ ) is in the direction of a classical moment characterizing the ground state. In the present case there are two such classical vectors in the direction of the canted moments (recall that we are considering only a single  $\text{CuO}_2$  plane). Therefore, we introduce two rotated coordinate systems, as shown in Fig. 2. Spin degrees of freedom in the initial representation are denoted by  $\mathbf{S}_{i\mathbf{g}}$ , but in the characteristic representation we use  $\mathbf{f}_{i\mathbf{g}}$ . (We follow the notation that  $i$ -sites belong to sublattice 1, whereas  $j$ -sites belong to sublattice 2.) For the sites of sublattice 1 we apply a transformation of the form

$$\begin{aligned} \begin{pmatrix} x \\ y \\ z \end{pmatrix}_i A &= \frac{1}{2} \begin{pmatrix} \sin \theta + 1 & \sin \theta - 1 \\ \sin \theta - 1 & \sin \theta + 1 \\ p \frac{\cos \theta}{2} & p \frac{\cos \theta}{2} \end{pmatrix} \begin{pmatrix} p \frac{\cos \theta}{2} & 1 & 0 \\ p \frac{\cos \theta}{2} & 0 & 1 \\ 2 \sin \theta & 0 & 0 \end{pmatrix} \begin{pmatrix} 1 \\ 0 \\ 0 \end{pmatrix} \begin{pmatrix} S_i^x \\ S_i^y \\ S_i^z \end{pmatrix} \\ &= \frac{1}{2} \begin{pmatrix} 1 & \sin \theta & \cos \theta \\ 0 & 1 & \cos \theta \\ 0 & p \frac{\sin \theta}{2} & p \frac{\sin \theta}{2} \end{pmatrix} \begin{pmatrix} S_i^x \\ S_i^y \\ S_i^z \end{pmatrix} A; \end{aligned} \quad (5)$$

and for sublattice 2

$$\begin{pmatrix} x \\ y \\ z \end{pmatrix}_j A = \frac{1}{2} \begin{pmatrix} 1 & \sin \theta & \cos \theta \\ 0 & 1 & \cos \theta \\ 0 & p \frac{\sin \theta}{2} & p \frac{\sin \theta}{2} \end{pmatrix} \begin{pmatrix} S_j^x \\ S_j^y \\ S_j^z \end{pmatrix} A; \quad (6)$$

The quantization axes ( $z$ ) of the new spin operators  $\mathbf{f}_i$  and  $\mathbf{f}_j$  coincide with the unit vectors in the direction of canted moments in Fig. 2.

The model Hamiltonian of Eq. (1) in terms of the new operators reads

$$\begin{aligned} H_{\text{CR}} &= \sum_{\langle i,j \rangle_{ab}} A (\mathbf{f}_i^+ \cdot \mathbf{f}_j + \mathbf{f}_i \cdot \mathbf{f}_j^+) + B \mathbf{f}_i^+ \cdot \mathbf{f}_j^+ \\ &\quad + \sum_{\langle i,j \rangle_{ac}} A (\mathbf{f}_i^+ \cdot \mathbf{f}_j + \mathbf{f}_i \cdot \mathbf{f}_j^+) + B \mathbf{f}_i^+ \cdot \mathbf{f}_j^+ \\ &\quad + \sum_{\langle i,j \rangle_{bc}} A (\mathbf{f}_i^+ \cdot \mathbf{f}_j + \mathbf{f}_i \cdot \mathbf{f}_j^+) + B \mathbf{f}_i^+ \cdot \mathbf{f}_j^+; \end{aligned} \quad (7)$$

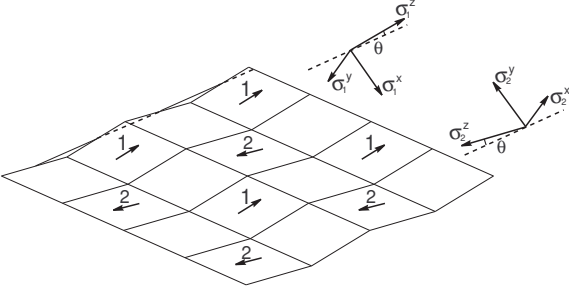


FIG. 2: Numbered arrows represent the Cu spin structure in a  $\text{CuO}_2$  plane. Two sublattices 1 and 2 are introduced. For each sublattice the spin coordinate system within the characteristic representation (i.e. after the transformations given by (5) and (6)) is shown. The thin net is shown only to simplify the visualization of the spin structure.

where we introduced the following definitions

$$\begin{aligned} J_1 &= J + \frac{r}{d^2} \frac{1}{2} (j_1 + j_3)^2; \\ J_2 &= \frac{1}{2} (j_1 + j_3) + \frac{r}{d^2} \frac{1}{2} (j_1 + j_3)^2; \\ J_3 &= \frac{1}{2} (j_1 + j_3) + \frac{r}{d^2} \frac{1}{2} (j_1 + j_3)^2; \\ J_4 &= \frac{d}{2} \sin \theta + \frac{r}{2} \cos \theta; \end{aligned} \quad (8)$$

$$A = \frac{J_1 - J_3}{4}; \quad B = \frac{J_4}{2} + i \frac{J_1 + J_3}{4}; \quad (9)$$

The subscripts  $hi$ ;  $ji_{ab}$  and  $hi$ ;  $ji_{ac}$  in the summations of Eq. (7) imply the nearest neighbours in the  $ab$  and  $ac$  directions, as shown in Fig. 1(b).

The form of the Hamiltonian in the characteristic representation is similar to an XYZ model, but is clearly more complicated since terms of the form  $\sum_{i,j} \sigma_i^x \sigma_j^y$  are present, which thus imply terms like  $\sigma_i^x \sigma_j^y$ . Thus, we can extract from our results, in this representation, the magnetic susceptibility of the XYZ calculated in both the mean-field and random phase approximations, by setting the imaginary part  $B = 0$ . We will consider numerical results for this simpler model in a future publication.

### C. Magnetic susceptibility in the initial and characteristic representations

We consider the response of the system, described by the Hamiltonian  $H$  in either the initial (Eq. (1)) or characteristic representation (Eq. (7)), to an externally applied constant magnetic field  $h$ . It is convenient to consider the application of this field in one direction only, which we take to be the direction of the initial repre-

sentation,

$$H^0 = H - h \sum_{l=1}^N S_l; \quad (10)$$

where  $\alpha = x$  or  $y$  or  $z$ , it is to be noted that  $\alpha$  is not summed over in Eq. (10), and  $N$  is the number of the lattice sites.

The statistical operator of the system is required to evaluate ensemble averages of relevant physical quantities, notably correlators and thermal Green's functions, and can be written as

$$Z = \text{Tr} e^{-H^0} = \text{Tr} e^{-H} T \exp \left( h \sum_{l=1}^N S_l \right); \quad (11)$$

where  $S_l(\alpha) = e^{i\alpha S_l} S_l e^{-i\alpha S_l}$  is the operator in the Heisenberg representation for imaginary time argument  $\alpha$ , and  $T$  is the time-ordering operator. The zero-field susceptibility describes the response of the system to such a field, and is defined to be

$$\frac{\partial \langle H \rangle}{\partial h} \bigg|_{h=0} = \frac{1}{N} \sum_{l=1}^N \sum_{l'=1}^N \langle S_l(\alpha) S_{l'}(0) \rangle; \quad (12)$$

where

$$\langle H \rangle = \frac{1}{N} \sum_{l=1}^N \langle S_l \rangle; \quad (13)$$

with correlators such as  $\langle S_l(\alpha) S_{l'}(0) \rangle$  taken with respect to the zero-field Hamiltonian  $H$ .

The square lattice is bipartite and can be divided into sublattices 1 and 2. Then, by using the definitions

$$\chi_{11} = \frac{2}{N} \sum_{i=1}^N \sum_{j=1}^N \langle S_i(\alpha) S_j(0) \rangle; \quad (14)$$

$$\chi_{22} = \frac{2}{N} \sum_{j=1}^N \sum_{i=1}^N \langle S_j(\alpha) S_i(0) \rangle; \quad (15)$$

$$\chi_{12} = \frac{2}{N} \sum_{i=1}^N \sum_{j=1}^N \langle S_i(\alpha) S_j(0) \rangle; \quad (16)$$

$$\chi_{21} = \frac{2}{N} \sum_{j=1}^N \sum_{i=1}^N \langle S_j(\alpha) S_i(0) \rangle; \quad (17)$$

where

$$i, j \in \text{sublattice 1}; \quad j, i \in \text{sublattice 2}$$

we can express the quantity of interest,  $\chi$ , as

$$\chi = \frac{1}{2} (\chi_{11} + \chi_{22} + \chi_{12} + \chi_{21}); \quad (18)$$



Then, using symmetry equivalent this simplifies (see below) the calculation of the zero-field susceptibility in the initial representation to

$$\chi_{11} = \chi_{11} + \chi_{12} : \quad (19)$$

The simpler form of Eq. (7) vs. Eq. (1) makes clear that it is desirable to perform calculations first using the characteristic representation, and to then transform back into the initial representation. To this end we require the relevant form of the susceptibility tensor in the characteristic representation. To begin, let us perform transformations  $S_1 = A^{-1}$ ,  $S_2 = B^{-1}$  ( $A = [a_{ij}]$ ,  $B = [b_{ij}]$ ) to the characteristic representation, such that the analogue of Eq. (10) is

$$H^0 = H_{CR} \sum_{i=1}^{N/2} (a_x x_i + a_y y_i + a_z z_i) h_1 + \sum_{j=1}^{N/2} (b_x x_j + b_y y_j + b_z z_j) h_2 : \quad (20)$$

Note that we have generalized the applied field to be  $h_1$  for sublattice 1, and  $h_2$  for sublattice 2, and in general we will treat these as two independent applied fields. If we define the components of susceptibility in the characteristic representation as

$$\chi_{11}^0 = \frac{2}{N} \sum_{i=1}^{N/2} \sum_{j=1}^{N/2} h \Gamma_{ij}(\vec{r}) \chi_{ij}^0(0) \text{id} ; \quad (21)$$

$$\chi_{12}^0 = \frac{2}{N} \sum_{i=1}^{N/2} \sum_{j=1}^{N/2} h \Gamma_{ij}(\vec{r}) \chi_{ij}^0(0) \text{id} ; \quad (22)$$

then the susceptibility given in Eq. (14) (N.B. in the initial representation) can be written as

$$\begin{aligned} \chi_{11} &= \frac{2}{N} \sum_{i=1}^{N/2} \frac{\partial \langle S_i \rangle}{\partial h_1} \\ &= \frac{2}{N} \sum_{i=1}^{N/2} a_x \frac{\partial \langle h_i^x \rangle}{\partial h_1} + a_y \frac{\partial \langle h_i^y \rangle}{\partial h_1} + a_z \frac{\partial \langle h_i^z \rangle}{\partial h_1} \\ &= a_x^2 \chi_{11}^{xx} + a_x a_y \chi_{11}^{xy} + a_x a_z \chi_{11}^{xz} \\ &+ a_y^2 \chi_{11}^{yy} + a_y a_x \chi_{11}^{yx} + a_y a_z \chi_{11}^{yz} \\ &+ a_z^2 \chi_{11}^{zz} + a_z a_x \chi_{11}^{zx} + a_z a_y \chi_{11}^{zy} ; \quad (23) \end{aligned}$$

and, in the same way (see Eq. (19))

$$\begin{aligned} \chi_{12} &= a_x b_x \chi_{12}^{xx} + a_x b_y \chi_{12}^{xy} + a_x b_z \chi_{12}^{xz} \\ &+ a_y b_y \chi_{12}^{yy} + a_y b_x \chi_{12}^{yx} + a_y b_z \chi_{12}^{yz} \\ &+ a_z b_z \chi_{12}^{zz} + a_z b_x \chi_{12}^{zx} + a_z b_y \chi_{12}^{zy} : \quad (24) \end{aligned}$$

The quantities  $\chi_{ij}^0$  that are introduced above in Eqs. (21,22) have the following interpretation. For instance, the component  $\chi_{12}^{xy}$  determine the response of the expectation value  $2 \sum_{i=1}^{N/2} \langle h_i^x \rangle$  of the spins of sublattice 1 to the magnetic field applied to the spins of sublattice 2 (no field applied to the spins of sublattice 1) in the  $y$  direction. Indeed, the perturbation  $H^0 = H_2 \sum_{j=1}^{N/2} h_j^y$  formally leads to the response

$$\frac{2}{N} \frac{\partial}{\partial h_2^y} \sum_{i=1}^{N/2} \langle h_i^x \rangle = \frac{2}{N} \sum_{i=1}^{N/2} \sum_{j=1}^{N/2} h \Gamma_{ij}(\vec{r}) \chi_{ij}^{xy}(0) \text{id} \chi_{12}^{xy} : \quad (25)$$

Similarly, the response of the spins of sublattice 1 to the perturbation  $H^0 = H_1 \sum_{i=1}^{N/2} h_i^y$  is given by

$$\frac{2}{N} \frac{\partial}{\partial h_1^y} \sum_{i=1}^{N/2} \langle h_i^x \rangle = \frac{2}{N} \sum_{i=1}^{N/2} \sum_{j=1}^{N/2} h \Gamma_{ij}(\vec{r}) \chi_{ij}^{xy}(0) \text{id} \chi_{11}^{xy} : \quad (26)$$

So, by substituting the inverse to the CR transformation, given by Eqs. (5,6), into Eqs. (23,24), and taking into account that  $\chi_{xx} = \chi_{yy} = \chi_{zz} = \chi_{xy} = \chi_{yz} = \chi_{zx} = 0$  in the

characteristic representation (which can be derived analytically), one obtains the desired transformation between the two representations, namely

$$x = \frac{x_{11}}{2} + \frac{x_{12}}{2} = \frac{1}{2} ( \frac{x_{11}^x}{2} + \frac{x_{12}^x}{2} + \frac{y_{11}^y}{2} + \frac{y_{12}^y}{2} + \frac{x_{11}^y}{2} + \frac{x_{12}^y}{2} + \frac{y_{11}^x}{2} + \frac{y_{12}^x}{2} ); \quad (27)$$

$$y = \frac{y_{11}}{2} + \frac{y_{12}}{2} = \frac{\sin^2(\theta)}{2} ( \frac{x_{11}^x}{2} + \frac{x_{12}^x}{2} + \frac{y_{11}^y}{2} + \frac{y_{12}^y}{2} + \frac{x_{11}^y}{2} + \frac{x_{12}^y}{2} + \frac{y_{11}^x}{2} + \frac{y_{12}^x}{2} ) + \cos^2(\theta) ( \frac{z_{11}^z}{2} + \frac{z_{12}^z}{2} ); \quad (28)$$

$$z = \frac{z_{11}}{2} + \frac{z_{12}}{2} = \frac{\cos^2(\theta)}{2} ( \frac{x_{11}^x}{2} + \frac{x_{12}^x}{2} + \frac{y_{11}^y}{2} + \frac{y_{12}^y}{2} + \frac{x_{11}^y}{2} + \frac{x_{12}^y}{2} + \frac{y_{11}^x}{2} + \frac{y_{12}^x}{2} ) + \sin^2(\theta) ( \frac{z_{11}^z}{2} + \frac{z_{12}^z}{2} ); \quad (29)$$

### III. MEAN FIELD ANALYSIS

In this section we develop the mean field approximation (MFA) for the system defined by Eq. (1), and obtain the behaviour of the magnetic susceptibility and a defining equation for the order parameter as a function of temperature. In part we include this derivation to make evident how the formalism of xIIC is applied to extract the zero-field uniform magnetic susceptibility. However, and more importantly, we will show that when the canting angle induced by the DM couplings is small, there are significant deviations from the mean-field results, viz. quantum fluctuation effects are large. Thus, here we establish the MFA susceptibility with which to make these comparisons.

Within the MFA we focus on one of the spins and replace its interaction with other spins by an effective field. To this end the following replacement is used:

$$S_i^a S_j^b = h_{ij}^a S_j^b + S_i^a h_{ij}^b - h_{ij}^a h_{ij}^b; \quad (30)$$

where a and b can be equal to any of x,y,z. It is to be noted that it is more convenient to perform the MFA calculations starting from the model in the characteristic representation, and thus we consider Eq. (7) and the analogue of the above equation for the operators.

First, we find the equation for the order parameter. The Hamiltonian Eq. (7) within the MFA reads as

$$H_i^{MFA} = -Z J_2 h_i^z; \quad (31)$$

and we find that the order parameter, to be denoted by  $\langle S_i^z \rangle$ , is found from the solution of

$$h_i^z = \frac{1}{2} \tanh \left( \frac{Z J_2}{2} \langle S_i^z \rangle \right); \quad (32)$$

where  $J_2$  is given by Eq. (8), and  $Z$  is the coordination number. From this equation it is immediately seen that within the MFA the Neel temperature at which  $\langle S_i^z \rangle$  vanishes is

$$T_N^{MFA} = J_2 = \frac{1}{2} ( \frac{1}{d^2} + \frac{1}{2} ) + \frac{1}{2} ( d^2 + 2 ) + [ J + \frac{1}{2} ( \frac{1}{d^2} + \frac{1}{2} ) ]^2 \quad (33)$$

Now, we find the susceptibility of the system within the MFA below  $T_N^{MFA}$ . First, we apply a magnetic field in the z direction of the sublattice 1

$$H^0 = H - \sum_i h_i^z; \quad \text{i-sites 2 1 sublattice:} \quad (34)$$

The Hamiltonian within the MFA can be written as

$$H^{MFA} = \sum_i \sum_j J_{ij} h_i^z h_j^z + \sum_i h_i^z \sum_j h_{ij}^z; \quad (35)$$

where  $\sum_{h_{ij}^z}$  means sum over all sites i which are nearest neighbours of site j. Then

$$h_i^z = \frac{1}{2} \tanh \left( \frac{1}{2} \sum_j J_{ij} h_j^z + h_i^z \right); \quad (36)$$

We write the mean value of  $h_i^z$  operators in the form

$$h_i^z = h_1^z + h_2^z; \quad h_j^z = h_1^z + h_2^z; \quad (37)$$

where  $h_1^z = h_2^z = \langle h_i^z \rangle$ , is the expectation value of  $h_i^z$  operator in the absence of the field, and the term  $h_2^z$  is the part of  $h_i^z$  induced by the applied field. Since the applied field  $h_1^z$  as well as the terms involving  $h_2^z$  are small, we may expand Eq. (36) in powers of these terms. Then, we find

$$\begin{aligned} h_1^z &= \frac{1}{2} \tanh \left( \frac{1}{2} \sum_j J_{ij} h_j^z + h_1^z \right) = \frac{1}{2} \tanh \left( \frac{1}{2} \sum_j J_{ij} h_1^z + h_1^z \right) + \frac{1}{2} \tanh \left( \frac{1}{2} \sum_j J_{ij} h_2^z \right); \\ h_2^z &= \frac{1}{2} \tanh \left( \frac{1}{2} \sum_j J_{ij} h_j^z + h_2^z \right) = \frac{1}{2} \tanh \left( \frac{1}{2} \sum_j J_{ij} h_1^z + h_2^z \right) + \frac{1}{2} \tanh \left( \frac{1}{2} \sum_j J_{ij} h_2^z \right); \end{aligned} \quad (38)$$

Due to the complicated couplings found in Eq. (7), the transverse components are much more involved to

calculate. Applying a field in the x direction to the spins of sublattice 1 we consider

$$H^0 = H \sum_i h_1^x \sigma_i^x; \quad i\text{-sites 2 1-sublattice}; \quad (39)$$

and within the MFA we thus examine

$$H^{0MFA} = \sum_i (h_1^x + h_1^x) \sigma_i^x + h_1^y \sigma_i^y + h_1^z \sigma_i^z \\ \sum_j (h_2^x \sigma_j^x + h_2^y \sigma_j^y + h_2^z \sigma_j^z); \quad (40)$$

Similarly, by applying a field in the y direction to the spins of sublattice 1 we consider

$$H^{0MFA} = \sum_i (h_1^x \sigma_i^x + [h_1^y + h_1^y] \sigma_i^y + h_1^z \sigma_i^z) \\ \sum_j (h_2^x \sigma_j^x + h_2^y \sigma_j^y + h_2^z \sigma_j^z); \quad (41)$$

where

$$h_1^x = \sum_i f - 2A h_j^x i + 2B h_j^y i g; \\ h_2^x = \sum_i f - 2A h_i^x i + 2B h_i^y i g; \\ h_1^y = \sum_i f - 2A h_j^y i + 2B h_j^x i g; \\ h_2^y = \sum_i f - 2A h_i^y i + 2B h_i^x i g; \\ h_1^z = \sum_j J_2 h_j^z i; \quad h_2^z = \sum_i J_2 h_i^z i;$$

where  $\text{Im} B$  denotes the imaginary part of  $B$ . Then, the system of equations determining the transverse components of susceptibility Eq. (25) and Eq. (26) within the MFA scheme is found to be

$$\frac{J_2}{2} \chi_{11}^{xx} = A \chi_{21}^{xx} = B \chi_{21}^{yx} \frac{1}{2Z}; \\ \frac{J_2}{2} \chi_{21}^{xx} = A \chi_{11}^{xx} = B \chi_{11}^{yx}; \\ \frac{J_2}{2} \chi_{11}^{yx} = A \chi_{21}^{yx} = B \chi_{21}^{xx}; \\ \frac{J_2}{2} \chi_{21}^{yx} = A \chi_{11}^{yx} = B \chi_{11}^{xx}; \\ \frac{J_2}{2} \chi_{11}^{xy} = A \chi_{21}^{xy} = B \chi_{21}^{yy}; \\ \frac{J_2}{2} \chi_{21}^{xy} = A \chi_{11}^{xy} = \frac{Z}{4} B \chi_{11}^{yy}; \\ \frac{J_2}{2} \chi_{11}^{yy} = A \chi_{21}^{yy} = B \chi_{21}^{xy} \frac{1}{2Z}; \\ \frac{J_2}{2} \chi_{21}^{yy} = A \chi_{11}^{yy} = B \chi_{11}^{xy}; \quad (42)$$

The solution of this system s, Eq. (42) turns out to be

$$\chi_{11}^{xx} = \chi_{22}^{xx} = \chi_{11}^{yy} = \chi_{22}^{yy} = \frac{J_2=2+A}{4Z \chi_1^2} + \frac{J_2=2-A}{4Z \chi_2^2}; \\ \chi_{12}^{xx} = \chi_{21}^{xx} = \chi_{12}^{yy} = \chi_{21}^{yy} = \frac{J_2=2+A}{\chi_1^2} \frac{J_2=2-A}{4Z \chi_2^2}; \\ \chi_{11}^{xy} = \chi_{22}^{xy} = \chi_{11}^{yx} = \chi_{22}^{yx} = \frac{B}{4Z} \frac{1}{\chi_1^2} \frac{1}{\chi_2^2}; \\ \chi_{12}^{xy} = \chi_{21}^{xy} = \chi_{12}^{yx} = \chi_{21}^{yx} = \frac{B}{4Z} \frac{1}{\chi_1^2} + \frac{1}{\chi_2^2}; \quad (43)$$

where

$$\chi_1 = \frac{q}{(J_2=2+A)^2} = B^2; \\ \chi_2 = \frac{q}{(J_2=2-A)^2} = B^2; \quad (44)$$

Using the relation between the components of susceptibility in the initial and characteristic representations given in Eqs. (27)–(29), we obtain the final result for zero-field uniform susceptibility within the MFA below the MFA ordering temperature,  $T_N^{MFA}$ , viz.

$$\chi^{MFA} = \frac{1}{4} \frac{1}{J_1 + J_2}; \quad (45) \\ \chi^{MFA} = \frac{1}{4} \frac{\sin^2(\theta)}{J_2 - J_3} + \frac{\cos^2(\theta)}{4} \frac{\text{sech}^2 \frac{n}{2} z J_2}{T + J_2 \text{sech}^2 \frac{n}{2} z J_2}; \quad (46) \\ \chi^{MFA} = \frac{1}{4} \frac{\cos^2(\theta)}{J_2 + J_3} + \frac{\sin^2(\theta)}{4} \frac{\text{sech}^2 \frac{n}{2} z J_2}{T - J_2 \text{sech}^2 \frac{n}{2} z J_2}; \quad (47)$$

with the equation for the order parameter given by Eq. (32). (For  $d = d_i = 0$ , implying that  $\theta = 0$  and  $J_2 = J$ , the above seemingly complicated results indeed reduce to the correct MFA expression for the susceptibility.)

The following comments on the MFA result are in order. First, note that for physical values of  $d$  and  $d_i$  ( $d; d_i \ll J$ ) the canting angle out of the xy plane is very small; thus, since the AF moment is in the yz plane and nearly aligned along the y axes,  $\chi^z$  diverges at  $T_N^{MFA}$ , but the other two components remain finite at the transition. However, while the x component of the susceptibility remains independent of temperature, since the canting produces a net FM moment in the z direction that is coupled to the y component of the local moment, there is an additional increase of  $\chi^y$  as the transition is approached from below.

Now consider the paramagnetic temperature region ( $T > T_N$ ), for which the only components with nonzero spin expectation values are those driven by the applied



eld. Following similar considerations to above, the final results for the components of susceptibility in the initial representation for high temperatures ( $T > T_N$ ) reads

$$\chi_{MFA}^x = \frac{1}{4} \frac{1}{J_1 + T}; \quad (48)$$

$$\chi_{MFA}^y = \frac{1}{4} \frac{\sin^2(\theta)}{T - J_3} + \frac{1}{4} \frac{\cos^2(\theta)}{T + J_2}; \quad (49)$$

$$\chi_{MFA}^z = \frac{1}{4} \frac{\cos^2(\theta)}{T + J_3} + \frac{1}{4} \frac{\sin^2(\theta)}{T - J_2}; \quad (50)$$

Note that in the limit  $T \rightarrow T_N^{MFA} = J_2$  we obtain that the  $x, y$  components of the susceptibility are continuous at the transition, whereas the  $z$  component of the susceptibility diverges at the Neel point, from above or below, owing to the presence of the weak ferromagnetic moment that first develops at the transition.

#### IV. LINEAR RESPONSE THEORY WITHIN THE RPA

##### A. Susceptibility below $T_N$

In this section we derive expressions for the static, uniform susceptibility within the RPA below the ordering temperature,  $T_N$ . Note that this temperature is determined with the RPA, and is not equivalent to that found in the previous section.

We employ thermal Green's functions in the analysis of the spin Hamiltonian given in Eq. (1) with spin  $\frac{1}{2}$ . The definition of such Green's functions for two Bose operators  $A, B$  and the corresponding equation of motion, are given by

$$G_{AB}(\omega) = \hbar T \langle A(\omega) B(0) \rangle; \quad (51)$$

$$\frac{dG_{AB}(\omega)}{d\omega} = \langle [A, B] \rangle + \hbar T \langle [H(\omega); A(\omega) B(0)] \rangle; \quad (52)$$

As discussed in the introduction, we adopt a procedure that was introduced by Liu,<sup>17</sup> as this technique allows for us to find longitudinal component of the susceptibility. To this end, we introduce the perturbed Hamiltonian (in the characteristic representation)

$$H_1^f = H_{CR} + \sum_i f \mathbf{h}_i^z; \quad (53)$$

where  $f$  is a small continuous field; note that the field is

applied to the spins of sublattice 1 only, and within the present paper we restrict  $f$  to be constant and static.

In the imaginary-time formalism, the Green's functions to be used are

$$G_{1n}^f(\omega) = \hbar T \langle \mathbf{h}_1^+(\omega) \mathbf{n}(0) \rangle i^f; \quad (54)$$

$$G_{1n}^f(\omega) = \hbar T \langle \mathbf{h}_1^-(\omega) \mathbf{n}(0) \rangle i^f; \quad \text{12 sublattice 1;}$$

$$G_{n^0n}^f(\omega) = \hbar T \langle \mathbf{h}_{n^0}^+(\omega) \mathbf{n}(0) \rangle i^f; \quad (54)$$

$$G_{n^0n}^f(\omega) = \hbar T \langle \mathbf{h}_{n^0}^-(\omega) \mathbf{n}(0) \rangle i^f; \quad \text{n2 sublattice 2;}$$

where the expectation values are taken with respect to the perturbed Hamiltonian in Eq. (53). After an expansion in a power series of  $f$  we can write

$$G_{1n}^f(\omega) = G_{1n}^{(0)}(\omega) + f G_{1n}^{(1)}(\omega) + O(f^2); \quad (55)$$

Since  $G_{1n}^{(0)}(\omega) = G_{1n}(\omega)$ , from now drop the superscript and use

$$G_{1n}^f(\omega) = G_{1n}(\omega) + f G_{1n}^{(1)}(\omega) + O(f^2); \quad (56)$$

Also, we introduce

$$\mathbf{h}_i^z(\omega) i^f = \mathbf{h}_i^z(\omega) + f \mathbf{v}_i + O(f^2); \quad (57)$$

where, due to the translation periodicity  $\mathbf{h}_i^z(\omega) = \mathbf{h}_{i+1}^z(\omega)$ , the order parameter at  $f = 0$ .

The equation of motion for the Green's function  $G_{1n}^f(\omega)$  is given by

$$\begin{aligned} \frac{dG_{1n}^f(\omega)}{d\omega} &= 2 \langle \mathbf{h}_1^z(\omega) \mathbf{h}_1^z(0) \rangle i^f \\ &+ \hbar T \langle [H_{CR}(\omega); \mathbf{h}_1^+(\omega) \mathbf{n}(0)] \rangle i^f - f G_{1n}^f(\omega); \end{aligned} \quad (58)$$

In order to solve this equation for the Green's function it must be linearized. We will use the random phase approximation (RPA), in which the fluctuations of  $\mathbf{h}_i^z$  are ignored and the operator  $\mathbf{h}_i^z$  is replaced by its mean value  $\langle \mathbf{h}_i^z \rangle$  — this is the so-called Tyablikov's decoupling.<sup>16</sup> For example

$$\begin{aligned} \hbar T \langle \mathbf{h}_1^z(\omega) \mathbf{h}_1^+(\omega) \mathbf{j} \rangle i^f &= \hbar T \langle \mathbf{h}_1^z(\omega) \mathbf{j} \rangle i^f \\ &+ \hbar T \langle \mathbf{h}_1^z(\omega) \mathbf{h}_1^+(\omega) \mathbf{j} \rangle i^f = \hbar T \langle \mathbf{h}_1^z(\omega) \mathbf{j} \rangle i^f G_{1j}^f(\omega); \end{aligned} \quad (59)$$

After this decoupling is introduced, Eq. (58) is found to be

$$\begin{aligned} \frac{dG_{1n}^f(\omega)}{d\omega} &= 2 \langle \mathbf{h}_1^z(\omega) \mathbf{h}_1^z(0) \rangle i^f + \sum_{ab} 2 \hbar T \langle \mathbf{h}_1^z(\omega) \mathbf{j} \rangle i^f [A_{(1+)_n}^f(\omega) B_{(1+)_n}^f(\omega) + J_2 \hbar T \langle \mathbf{h}_{1+}^z(\omega) \mathbf{j} \rangle i^f G_{1n}^f(\omega)] \\ &+ \sum_{ac} 2 \hbar T \langle \mathbf{h}_1^z(\omega) \mathbf{j} \rangle i^f [A_{(1+)_n}^f(\omega) + B_{(1+)_n}^f(\omega)] + J_2 \hbar T \langle \mathbf{h}_{1+}^z(\omega) \mathbf{j} \rangle i^f G_{1n}^f(\omega) - f G_{1n}^f(\omega); \end{aligned} \quad (60)$$

where  $\sum_{\mathbf{l} \in \mathbf{P}}^{\text{ab}}$  refers to a summation over the nearest neighbours of the site  $\mathbf{l}$  in the  $\text{ab}$  direction, and similarly for  $\sum_{\mathbf{l} \in \mathbf{P}}^{\text{ac}}$  (see Fig. 1(b)). Here, all sites  $\mathbf{l} \in \mathbf{P}$  belong to the sublattice 2.

We introduce the Fourier transformation in the momentum-frequency representation for the Green's function and the spin operator

$$G_{\mathbf{l}\mathbf{m}}^{\mathbf{f}}(\omega) = \frac{2}{N} \sum_{\mathbf{k}, \mathbf{m}} G_{12}^{\mathbf{f}}(\mathbf{k}; \mathbf{l}_m) e^{i\mathbf{k} \cdot (\mathbf{R}_1 - \mathbf{R}_m)} e^{-i\omega \mathbf{l}_m}; \quad (61)$$

$$\begin{aligned} h_{\mathbf{l}}^{\mathbf{z}}(\omega) \mathbf{f} &= \frac{1}{N} \sum_{\mathbf{k}, \mathbf{m}} h_{\mathbf{l}}^{\mathbf{z}}(\mathbf{k}; \mathbf{l}_m) i\mathbf{f} e^{i\mathbf{k} \cdot \mathbf{R}_1} e^{-i\omega \mathbf{l}_m} \\ &= \sum_{\mathbf{k}} (\mathbf{k}) [\mathbf{f} + \mathbf{f}_V] e^{i\mathbf{k} \cdot \mathbf{R}_1}; \end{aligned} \quad (62)$$

where the expansion in Eq. (57) and the linear response to the uniform perturbation expressed by  $v_1(\mathbf{k}) = (\mathbf{k})v_1$  were taken into account. In the transformation given by Eqs. (61,62), the sum over  $\mathbf{k}$  runs over  $\frac{1}{2}N$  points of the first zone in the momentum space, and  $\mathbf{l}_n = 2 - n$  for  $n = 2, 3, \dots, Z$  are the Bose Matsubara frequencies. Then, we can write down the equation for the Green's function  $G_{\mathbf{l}\mathbf{m}}^{\mathbf{f}}(\omega)$  in the form

$$\begin{aligned} i\mathbf{l}_m G_{12}^{\mathbf{f}}(\mathbf{k}; \mathbf{l}_m) &= \mathbf{f} G_{12}^{\mathbf{f}}(\mathbf{k}; \mathbf{l}_m) \\ &\quad + \frac{J_2}{2Z} [\mathbf{f} + \mathbf{f}_V] G_{12}^{\mathbf{f}}(\mathbf{k}; \mathbf{l}_m) \\ &\quad + 2Z A_k [\mathbf{f} + \mathbf{f}_V] G_{22}^{\mathbf{f}}(\mathbf{k}; \mathbf{l}_m) \\ &\quad + 2Z B_k [\mathbf{f} + \mathbf{f}_V] G_{22}^{\mathbf{f}}(\mathbf{k}; \mathbf{l}_m); \end{aligned} \quad (63)$$

where, as before,  $Z$  is the coordination number, and we introduce

$$\begin{aligned} A_k &= A_{\mathbf{k}}; \quad B_k = \langle B \rangle_k^0 + \langle B \rangle_k; \\ \mathbf{k} &= \frac{1}{2} (\cos k_x + \cos k_y); \quad \mathbf{k}^0 = \frac{1}{2} (\cos k_x - \cos k_y); \end{aligned} \quad (64)$$

From these we can write down the following two equations:

$$\frac{i\mathbf{l}_m}{2Z} G_{12} = \frac{J_2}{2} G_{12} + A_k G_{22} - B_k G_{22}; \quad (65)$$

$$\begin{aligned} \frac{i\mathbf{l}_m}{2Z} G_{12}^{(1)} &= \frac{1}{2Z} G_{12} \\ &\quad + \frac{v_2}{2} \frac{J_2}{2} G_{12} + \frac{J_2}{2} G_{12}^{(1)} + \frac{v_1}{2} A_k G_{22} + A_k G_{22}^{(1)} \\ &\quad - \frac{v_1}{2} B_k G_{22} - B_k G_{22}^{(1)}; \end{aligned} \quad (66)$$

where in all equations we drop the wave vector and frequency dependencies for the Green's functions, that is  $G = G(\mathbf{k}; \mathbf{l}_m)$  and  $G^{(1)} = G^{(1)}(\mathbf{k}; \mathbf{l}_m)$ .

In the same way we obtain the equations of motion for the other Green's functions (see Eq. (54)) within the RPA scheme. The final systems of equations for zeroth- and first-order quantities can be written as

$$\begin{aligned} \frac{i\mathbf{l}_m}{2Z} \frac{J_2}{2} G_{12} &= A_k G_{22} - B_k G_{22}; & \frac{i\mathbf{l}_m}{2Z} + \frac{J_2}{2} G_{12} &= A_k G_{22} + B_k G_{22}; \\ \frac{i\mathbf{l}_m}{2Z} \frac{J_2}{2} G_{22} &= A_k G_{12} - B_k G_{12} - \frac{1}{Z}; & \frac{i\mathbf{l}_m}{2Z} + \frac{J_2}{2} G_{22} &= A_k G_{12} + B_k G_{12}; \end{aligned} \quad (67)$$

$$\begin{aligned} \frac{i\mathbf{l}_m}{2Z} \frac{J_2}{2} G_{12}^{(1)} &= A_k G_{22}^{(1)} - B_k G_{22}^{(1)} + \frac{v_2}{2} \frac{J_2}{2} + \frac{v_1}{2} \frac{i\mathbf{l}_m}{2Z} \frac{J_2}{2} + \frac{1}{2Z} G_{12}; \\ \frac{i\mathbf{l}_m}{2Z} \frac{J_2}{2} G_{22}^{(1)} &= A_k G_{12}^{(1)} - B_k G_{12}^{(1)} + \frac{v_1}{2} \frac{J_2}{2} + \frac{v_2}{2} \frac{i\mathbf{l}_m}{2Z} \frac{J_2}{2} G_{22}; \\ \frac{i\mathbf{l}_m}{2Z} + \frac{J_2}{2} G_{12}^{(1)} &= A_k G_{22}^{(1)} + B_k G_{22}^{(1)} - \frac{v_2}{2} \frac{J_2}{2} - \frac{v_1}{2} \frac{i\mathbf{l}_m}{2Z} + \frac{J_2}{2} + \frac{1}{2Z} G_{12}; \\ \frac{i\mathbf{l}_m}{2Z} + \frac{J_2}{2} G_{22}^{(1)} &= A_k G_{12}^{(1)} + B_k G_{12}^{(1)} - \frac{v_1}{2} \frac{J_2}{2} - \frac{v_2}{2} \frac{i\mathbf{l}_m}{2Z} + \frac{J_2}{2} G_{22}; \end{aligned} \quad (68)$$

$$\begin{aligned}
\frac{i!_m}{2Z} - \frac{J_2}{2} G_{21}^{(1)} &= A_k G_{11}^{(1)} - B_k G_{11}^{(1)} + \frac{v_1 J_2}{2} + \frac{v_2}{2Z} \frac{i!_m}{2Z} - \frac{J_2}{2} G_{12}; \\
\frac{i!_m}{2Z} - \frac{J_2}{2} G_{11}^{(1)} &= A_k G_{21}^{(1)} - B_k G_{21}^{(1)} + \frac{v_2 J_2}{2} + \frac{v_1}{2Z} \frac{i!_m}{2Z} - \frac{J_2}{2} + \frac{1}{2Z} G_{22}; \\
\frac{i!_m}{2Z} + \frac{J_2}{2} G_{21}^{(1)} &= A_k G_{11}^{(1)} + B_k G_{11}^{(1)} - \frac{v_1 J_2}{2} - \frac{v_2}{2Z} \frac{i!_m}{2Z} + \frac{J_2}{2} G_{12}; \\
\frac{i!_m}{2Z} + \frac{J_2}{2} G_{11}^{(1)} &= A_k G_{21}^{(1)} + B_k G_{21}^{(1)} - \frac{v_2 J_2}{2} - \frac{v_1}{2Z} \frac{i!_m}{2Z} + \frac{J_2}{2} + \frac{1}{2Z} G_{22};
\end{aligned} \tag{69}$$

where we have taken into account the relations

$$\begin{aligned}
G_{12} &= G_{21}; \quad G_{11} = G_{22}; \\
G_{12} &= G_{21}; \quad G_{11} = G_{22};
\end{aligned} \tag{70}$$

The poles of the zero-order Green's functions  $G$  have to be the same as the poles found for the first-order ones  $G^{(1)}$ . This can be seen directly by comparing the structure of the systems of equations for the corresponding quantities: the system in Eq. (67) for the zero-order functions is identical with the systems in Eqs. (68,69) for the first-order ones, except for the free terms. The free terms in the first-order systems are determined by the zero-order Green's functions, thus, the first-order quantities  $G^{(1)}$  can be written down in terms of the solution for the zero-order system of Eq. (67), and the as yet unknown quantities  $v_1$  and  $v_2$ .

To calculate  $v_{1,2}$  we use a relation connecting  $v$  and the Green's functions  $G^{(1)}(k; 0)$ . From the definitions in Eq. (54) and the expansion in Eq. (57) we have

$$G_{ii}^f(0) = \frac{1}{2} \quad h_{ii}^{zf} = \frac{1}{2} \quad f_{ij} \tag{71}$$

while the expansion in Eq. (56) leads to

$$G_{ii}^f(0) = G_{ii}(0) + f G_{ii}^{(1)}(0) = \frac{1}{2} + f G_{ii}^{(1)}(0); \tag{72}$$

Thus, we can write down  $v_i = G_{ii}^{(1)}(0)$ , and after Fourier summation one obtains

$$v_1 = \frac{2}{N} \sum_k G_{11}^{(1)}(k; 0); \tag{73}$$

$$v_2 = \frac{2}{N} \sum_k G_{22}^{(1)}(k; 0); \tag{74}$$

The solution of the system in Eq. (68) gives us the first-order Green's function  $G_{22}^{(1)}(k; i!_m)$  and therefore  $v_2$ . Similarly, to find  $v_1$  we use Eq. (69).

The solution of the system of equations in Eq. (67) for the zeroth-order Green's functions turns out to be

$$\begin{aligned}
G_{12}(k; i!_n) &= \frac{1}{2} \left[ 1 + \frac{J_2=2+A_k}{i!_1(k)} \frac{1}{i!_n - i!_1(k)} + 1 \frac{J_2=2+A_k}{i!_1(k)} \frac{1}{i!_n + i!_1(k)} \right. \\
&\quad \left. + 1 + \frac{J_2=2-A_k}{i!_2(k)} \frac{1}{i!_n - i!_2(k)} + 1 \frac{J_2=2-A_k}{i!_2(k)} \frac{1}{i!_n + i!_2(k)} \right]; \\
G_{22}(k; i!_n) &= \frac{1}{2} \left[ 1 + \frac{J_2=2+A_k}{i!_1(k)} \frac{1}{i!_n - i!_1(k)} + 1 \frac{J_2=2+A_k}{i!_1(k)} \frac{1}{i!_n + i!_1(k)} \right. \\
&\quad \left. + 1 + \frac{J_2=2-A_k}{i!_2(k)} \frac{1}{i!_n - i!_2(k)} + 1 \frac{J_2=2-A_k}{i!_2(k)} \frac{1}{i!_n + i!_2(k)} \right]; \\
G_{12}(k; i!_n) &= \frac{-B_k}{2} \left[ \frac{1}{i!_1(k)} \frac{1}{i!_n - i!_1(k)} \frac{1}{i!_n + i!_1(k)} + \frac{1}{i!_2(k)} \frac{1}{i!_n - i!_2(k)} \frac{1}{i!_n + i!_2(k)} \right]; \\
G_{22}(k; i!_n) &= \frac{-B_k}{2} \left[ \frac{1}{i!_1(k)} \frac{1}{i!_n - i!_1(k)} \frac{1}{i!_n + i!_1(k)} + \frac{1}{i!_2(k)} \frac{1}{i!_n - i!_2(k)} \frac{1}{i!_n + i!_2(k)} \right];
\end{aligned} \tag{75}$$

where the spectra for the out-of-plane  $\omega_1(k)$  and in-plane  $\omega_2(k)$  modes<sup>14</sup> are given by

$$\begin{aligned}\omega_1(k) &= 2Z \quad \omega_2(k) = 2Z \quad \frac{1}{\sqrt{(J_2=2 + A_k)^2 - B_k^2}}; \\ \omega_2(k) &= 2Z \quad \omega_1(k) = 2Z \quad \frac{1}{\sqrt{(J_2=2 - A_k)^2 - B_k^2}};\end{aligned}\quad (76)$$

After the substitution of the results in Eq. (75) into the system of equations in Eqs. (68,69), and then using the solutions for  $G_{11}^{(1)}(k; i_m)$ ,  $G_{22}^{(1)}(k; i_m)$ , the results for quantities  $v_1$  and  $v_2$  are found to be

$$v_1 - v_2 = \frac{2C_1}{1 + 4J_2C_1}; \quad (77)$$

$$v_1 + v_2 = \frac{2C_2}{1 - 8J_2C_3}; \quad (78)$$

where

$$\begin{aligned}C_1 &= \frac{2}{N} \sum_k \left( 1 + \frac{(J_2=2)^2 A_k^2 B_k^2}{\omega_1(k) \omega_2(k)} \frac{n(\omega_1)}{\omega_2(k)} \frac{n(\omega_2)}{\omega_1(k)} - 1 \frac{(J_2=2)^2 A_k^2 B_k^2}{\omega_1(k) \omega_2(k)} \frac{n(\omega_1) + n(\omega_2) + 1}{\omega_1(k) + \omega_2(k)} \right); \\ C_2 &= \frac{2}{N} \sum_k \left( \frac{(J_2=2 + A_k)^2 - 2}{\omega_1^2(k) \sinh^2 \frac{\omega_1}{2}} + \frac{B_k^2 [2n(\omega_1) + 1]}{\omega_1^2(k) \omega_2(k)} + \frac{(J_2=2 - A_k)^2 - 2}{\omega_2^2(k) \sinh^2 \frac{\omega_2}{2}} + \frac{B_k^2 [2n(\omega_2) + 1]}{\omega_2^2(k) \omega_1(k)} \right); \\ C_3 &= \frac{2}{N} \sum_k \left( \frac{(J_2=2 + A_k)^2 - 2}{\sinh^2 \frac{\omega_1}{2}} + \frac{(J_2=2 - A_k)^2 - 2}{\sinh^2 \frac{\omega_2}{2}} \right); \text{ here } n(\omega_{1,2}) = [\exp(-\omega_{1,2}(k)) - 1]^{-1};\end{aligned}\quad (79)$$

Now let us find the quantities which determine a linear response to a magnetic field applied to the one of sublattice { see Eqs. (25,26). The longitudinal  $z$  components of the susceptibility in the characteristic representation are given by

$$\chi_{11}^z = \frac{\partial \chi_{11}^z}{\partial f} \bigg|_{f=0} = v_1; \quad \chi_{12}^z = \frac{\partial \chi_{12}^z}{\partial f} \bigg|_{f=0} = v_2; \quad (80)$$

where the expansion of Eq. (57) was used. The transverse  $x$  and  $y$  components of the susceptibility tensor are determined in the terms of Green's functions as

$$\begin{aligned}\chi_{11}^0 &= \frac{2}{N} \sum_{i,j} \sum_k \text{Tr} \left( \rho_i(k) \rho_j(0) \right) id; \\ \chi_{12}^0 &= \frac{2}{N} \sum_{i,j} \sum_k \text{Tr} \left( \rho_i(k) \rho_j(0) \right) id;\end{aligned}\quad (81)$$

where  $\rho = x; y$ . By substituting the solutions in Eq. (75) into the definition in Eq. (81) for the transverse components of susceptibility, we easily obtain exactly the same result that we have already found within our MFA calculations { that is, Eq. (43).

Then, using Eqs. (27)–(29) the components of the susceptibility in the initial coordinate system of Eq. (1) are

found to be

$$\chi^x = \frac{1}{4} \frac{1}{J_1 + J_2}; \quad (82)$$

$$\chi^y = \frac{1}{4} \frac{\sin^2(\theta)}{J_2 - J_3} + \cos^2(\theta) [v_1 - v_2]; \quad (83)$$

$$\chi^z = \frac{1}{4} \frac{\cos^2(\theta)}{J_2 + J_3} + \sin^2(\theta) [v_1 + v_2]; \quad (84)$$

For completeness, we mention that we have also performed the theoretical investigation of this model (1) within spin-wave (SW) theory, and the final result for the components of static susceptibility turns out to be

$$\chi^{x \text{ SW}} = \frac{1}{4} \frac{1}{J_1 + J_2}; \quad (85)$$

$$\chi^{y \text{ SW}} = \frac{1}{4} \frac{\sin^2(\theta)}{J_2 - J_3} + \cos^2(\theta) S^2 C_1 - S; \quad (86)$$

$$\chi^{z \text{ SW}} = \frac{1}{4} \frac{\cos^2(\theta)}{J_2 + J_3} + \sin^2(\theta) S^2 C_2 - S; \quad (87)$$

It can be noted that the difference in the results within the RPA, Eqs. (82)–(84), and spin-wave theory, Eqs. (85)–(87), came from the calculation of the components of the susceptibility in the direction of the sublattice magnetization (that is  $\chi_{11}^z$  and  $\chi_{12}^z$ ). The spin-wave theory gives unity in the denominator of the expressions for  $\chi_{11}^z$  and  $\chi_{12}^z$  in Eq. (77), and  $S = 1/2$  instead of the order parameter everywhere in the numerator.

The similar situation takes place for antiferromagnetic Heisenberg model within the RPA scheme<sup>17</sup> and spin-wave theory.<sup>31</sup>

We also mention that the transverse components of the susceptibility in the characteristic representation (43) are equal within the MFA, RPA, and SW theories.

#### B. Related Thermodynamic quantities

In order for the above RPA theory to be complete, we need to determine the behaviour of the order parameter and the transition temperature.

The above expressions for the components of susceptibility Eqs. (83,84), and for the elementary excitations (spin waves) given by Eq. (76), include the as-yet-unknown value of the order parameter. From the definition on the Green's functions we can obtain

$$G_{nn}(\omega = 0) = \hbar \sum_n \frac{1}{\omega_n} ; \quad (88)$$

$$\text{where } G_{nn}(0) = \frac{2}{N} \sum_k X G_{22}(k; 0) ;$$

Substituting  $G_{22}(k; \omega)$  from Eq. (75), and performing the summation on the Matsubara frequencies, the equation on the order parameter turns out to be

$$\frac{1}{N} = \frac{2}{N} \sum_k \frac{J_2=2+A_k}{\omega_1(k)} [2n(\omega_1)+1] + \frac{J_2=2-A_k}{\omega_2(k)} [2n(\omega_2)+1] ; \quad (89)$$

Since order parameter (89) (sublattice magnetization) is temperature dependent, it follows that the spectrum of elementary excitations (Eq. (76)) is also temperature dependent.

The Neel temperature at which it vanishes within the adopted RPA approximation is determined by

$$T_N = \left( \frac{1}{4N} \sum_k \frac{J_2=2+A_k}{\omega_1^2(k)} + \frac{J_2=2-A_k}{\omega_2^2(k)} \right)^{-1} ; \quad (90)$$

By putting  $\omega \rightarrow 0$  we can find that z-component of susceptibility in Eq. (84)

$$\chi_z(\omega \rightarrow 0) = \frac{1}{4} \frac{\cos^2(\theta)}{J_2 + J_3} + \sin^2(\theta) \frac{TC_2 \chi_z(0)}{1 - T/T_N} ; \quad (91)$$

diverges at the Neel temperature, whereas other components of susceptibility remain finite as the Neel point is approached from below.

#### C. Susceptibility in the paramagnetic case

When the temperature of the system is above the Neel temperature,  $T_N$ , there still exists short-range magnetic order. To model such an order<sup>17</sup> we introduce a fictitious field pointing in the direction of the sublattice magnetization, that is the z direction in the characteristic representation. To this end, the Hamiltonian

$$H_h = H_{CR} - \sum_i \frac{X}{\hbar} \frac{z}{i} - \sum_j \frac{X}{\hbar} \frac{z}{j} \quad (92)$$

is used, and the limit  $\hbar \rightarrow 0$  is taken after the calculation is carried out. To obtain the susceptibility above the Neel temperature, it is convenient to introduce an order parameter defined by

$$y = \lim_{\hbar \rightarrow 0} (2Z - \hbar) ; \quad (93)$$

The calculations for the model are very similar to the ones above presented. It is easy to show that paramagnetic version of the equation on the order parameter in Eq. (89) leads to

$$\frac{1}{y} = \frac{2}{N} \sum_k \frac{1}{Z} \frac{1 + y(J_2=2+A_k)}{(1 + y(J_2=2+A_k))^2} \frac{1}{y^2 \beta_k^2} + \frac{1 + y(J_2=2-A_k)}{(1 + y(J_2=2-A_k))^2} \frac{1}{y^2 \beta_k^2} ; \quad (94)$$

The quantity  $y$  approaches to infinity as the temperature is lowered to  $T_N$ . Indeed, putting  $y \rightarrow 1$  in Eq. (94) we find the temperature at which  $y$  diverges, which is nothing but Neel temperature.

By a procedure similar to the above presented (that is, the RPA scheme below  $T_N$ ) the different components of the magnetic susceptibility in the paramagnetic phase are found to be

$$\chi_x = \frac{1}{4} \frac{1}{J_1 + J_2 + 2=y} ; \quad (95)$$

$$\chi_y = \frac{1}{4} \frac{\sin^2(\theta)}{J_2 - J_3 + 2=y} + \cos^2(\theta) \frac{y^2 D_1}{1 + 8y(1+yJ_2=2)D_1} ; \quad (96)$$

$$\chi_z = \frac{1}{4} \frac{\cos^2(\theta)}{J_2 + J_3 + 2=y} + \sin^2(\theta) \frac{y^2 D_2}{1 - 8y^2 D_3} ; \quad (97)$$

where



$$\begin{aligned}
D_1 &= \frac{1}{2Z^2} \frac{2}{N_k} X \frac{(1+y(J_2=2+A_k))(1+y(J_2=2-A_k))}{f(1+y(J_2=2+A_k))^2} \frac{y^2 \beta_k f}{y^2 \beta_k f g f(1+y(J_2=2-A_k))^2} \frac{y^2 \beta_k f}{y^2 \beta_k f g}; \\
D_2 &= \frac{1}{2Z^2} \frac{2}{N_k} X \frac{(1+y(J_2=2+A_k))^2 + y^2 \beta_k f}{f(1+y(J_2=2+A_k))^2} \frac{y^2 \beta_k f}{y^2 \beta_k f g^2} + \frac{(1+y(J_2=2-A_k))^2 + y^2 \beta_k f}{f(1+y(J_2=2-A_k))^2} \frac{y^2 \beta_k f}{y^2 \beta_k f g^2}; \\
D_3 &= \frac{1}{2Z^2} \frac{2}{N_k} X \frac{1+y(J_2=2+A_k)}{(1+y(J_2=2+A_k))^2} \frac{1}{y^2 \beta_k f} + \frac{1+y(J_2=2-A_k)}{(1+y(J_2=2-A_k))^2} \frac{1}{y^2 \beta_k f};
\end{aligned} \tag{98}$$

By putting  $y \rightarrow 1$  we obtain that the components of susceptibility  $\chi^x$  and  $\chi^y$  are continuous at the Neel point, whereas the z-component of susceptibility diverges in the  $y \rightarrow 1$  limit at the Neel point, the latter result reflecting the presence of the spontaneous canted ferromagnetic moment in the z direction.

D. Susceptibility in the  $T = 0$  limit

As we will present in the results discussion, the dimensionality of the parameter space that seems to be relevant to the cuprates is large, but there are only a few important values that determine the physical properties of the system. Here we discuss two key experimentally obtainable quantities, and their relation to the above theory.

It has been reported, using inelastic neutron scattering, that the out-of-plane ( $\chi_1$ ) and in-plane ( $\chi_2$ ) spin-wave gaps are 5.0 and 2.3 meV, respectively, in the LTO phase of  $\text{La}_2\text{CuO}_4$  crystal.<sup>5</sup> Using these results let us predict the ratio of the components of susceptibility  $\chi^y = \chi^x$ . The zone-centre ( $k = 0$ ) spin-wave gaps are given by

$$\begin{aligned}
\chi_1 &= Z \frac{P}{(J_2 + J_1)(J_2 - J_3)}; \\
\chi_2 &= Z \frac{P}{(J_2 - J_1)(J_2 + J_3)};
\end{aligned} \tag{99}$$

and they are real if  $J_2 < J_1, J_3$ . So, from these relations we obtain

$$\chi_2 < \chi_1, \quad J_1 > J_3; \tag{100}$$

Also, in the  $T = 0$  limit the y component of the susceptibility in Eq. (46) is given by

$$\begin{aligned}
\chi_{y \text{ MFA}} &= \frac{1}{4} \frac{\sin^2(\theta)}{J_2 - J_3} = \frac{1}{4} \frac{J_2}{J_2^2} \frac{J_1}{J_3^2}; \\
\text{then } \frac{\chi_{y \text{ MFA}}}{\chi_{x \text{ MFA}}} &= \frac{J_2^2}{J_2^2} \frac{J_1^2}{J_3^2};
\end{aligned} \tag{101}$$

Therefore, within the MFA

$$\chi_{x \text{ MFA}} > \chi_{y \text{ MFA}}, \quad J_1 > J_3; \tag{102}$$

Thus, if  $\chi_2 < \chi_1$  ( $\chi_2 > \chi_1$ ), in the limit of zero temperature the MFA predicts that  $\chi^y < \chi^x$  ( $\chi^y > \chi^x$ ).

In the limit of the small anisotropy  $d; J$  the components of the susceptibility at  $T = 0$  within the MFA turn out to be

$$\begin{aligned}
\chi_{x \text{ MFA}} &= \chi_{z \text{ MFA}} = \frac{1}{8J}; \\
\chi_{y \text{ MFA}} &= \frac{d^2}{32J^2(\chi_1 - \chi_3)};
\end{aligned} \tag{103}$$

while the expressions for the spin-wave gaps are

$$\chi_1 = Z \frac{P}{2J(\chi_1 - \chi_3)}; \quad \chi_2 = Z \frac{P}{d^2 - 2}; \tag{104}$$

We can see that components  $\chi^{x/z}$  are almost independent of the anisotropy parameters, while the  $\chi^y$  component is very sensitive to the ratio between the anti-symmetric  $d$  and symmetric  $\chi_1 - \chi_3$  parameters of anisotropy. Then, the ratio between the components of the susceptibility is given by

$$\frac{\chi_{x/z \text{ MFA}}}{\chi_{y \text{ MFA}}} = \frac{\chi_1^2}{\chi_2^2}; \tag{105}$$

It can be noted that within the MFA scheme the different components of the susceptibility, i.e.  $\chi^x$ ,  $\chi^y$  and  $\chi^z$ , are determined by the contributions from the transverse components of the susceptibility in the characteristic representation. Indeed, as should be expected, the longitudinal components of the susceptibility in the CR (see Eq. (38)) are equal to zero in the  $T = 0$  limit. As showed earlier in this paper, in the characteristic representation the RPA and SW theories lead to the same result for the transverse components of the susceptibility as the MFA does. Since the longitudinal components in the CR, given by the Eq. (77) within the RPA, and their simplified expressions within the SW theory (see Eqs. (86,87)) become negligibly small in the  $T = 0$  limit, we predict that RPA, SW and MFA within the reasonable range of the model parameters ( $d; J$ ) satisfy the ratio of Eq. (105), and the different components of the susceptibility at  $T = 0$  can be approximated by the Eq. (103).

We also note the analogy with the pure 3D Heisenberg model where, in the limit of zero temperature, all approximations considered here give the same magnitude

for the transverse components of the susceptibility, and zero for the longitudinal one.<sup>17</sup>

## V. RESULTS OF CALCULATIONS

In this section we present the results of a numerical investigation of the magnetic properties of the system modelled by the Hamiltonian given by Eq. (1) based on the above presented analytical formulae. Specifically, we are interested in the temperature dependencies of the various components of the susceptibility for different values (specifically, ratios) of the model parameters. Further, we will numerically demonstrate the correlation between the magnitudes of the two spin-wave gaps in the excitation spectrum and the behaviour of the susceptibility components; this relation was discussed analytically in the previous subsection. Also, and most importantly, we will make clear the role played by quantum fluctuations by comparing the results of the different approximation schemes.

In what follows, we will mainly examine one set of parameters that are suggested from experimental measurements discussed in the previous subsection, and this will allow us to "zero in" on a parameter regime. However, since we have developed the theory for one plane and not a 3d solid, we do not necessarily expect this set of parameters to be representative of a system like  $\text{La}_2\text{CuO}_4$ ; instead, as we discussed in the introduction to this paper, this approach will allow us to determine if a one-plane approach is adequate, since, as we and others have discussed, a true  $T_c > 0$  phase transition is possible for one plane and thus could possibly be sufficient for this system.

In the present calculations we express all model parameters in terms of  $J$ . Also, as will be made clear below, instead of using the set of parameters  $\epsilon_1$ ,  $\epsilon_2$ , and  $\epsilon_3$ , we deal with combination of parameters  $\epsilon_1 - \epsilon_3$ ,  $\epsilon_1 + \epsilon_3$ , and  $\epsilon_2$ . The chosen magnitudes of the model parameters  $d$  and  $\epsilon_1 - \epsilon_3$  give the reported magnitude of gaps in the spectrum<sup>5,32</sup>

$$\epsilon_0 = \epsilon_1 - \epsilon_3 = 5 \text{ meV}; \quad \epsilon_1 = \epsilon_2 = 2.3 \text{ meV}; \quad (106)$$

at the temperature  $T = T_N = 3$  for the superexchange value  $J = 130 \text{ meV}$ .<sup>5</sup> This leads to the parameters given by

$$d/J = 0.02; \quad (\epsilon_1 - \epsilon_3)/J = 0.42 \cdot 10^{-3}; \quad (107)$$

where, as discussed below, we have set

$$(\epsilon_1 + \epsilon_3)/J = 0; \quad \epsilon_2 = 0; \quad (108)$$

### A. The AFM order parameter, spin-wave excitations, and $T_N$

To examine the different analytical schemes used in the previous sections, we compare the representative solutions of the order parameter,  $\eta$ , within the RPA method,

Eq. (89), and within the MFA, Eq. (32). Most interestingly, we note the results shown in Fig. 3(a) look very similar to the corresponding ones for the pure 3D quantum Heisenberg antiferromagnet within the RPA and MFA schemes.<sup>16</sup>

Since the order parameter is temperature dependent, it follows that within the RPA scheme the spin-wave spectrum (see Eq. (76)) is also temperature dependent. In Fig. 3(b) we present the behaviour of both modes in the excitation spectrum at the long wavelength limit ( $k = 0$ ) (energy gaps) with respect to the relative temperature ( $T = T_N$ ); these results compare favourably with the experimental measurements of the same quantity.<sup>5</sup>

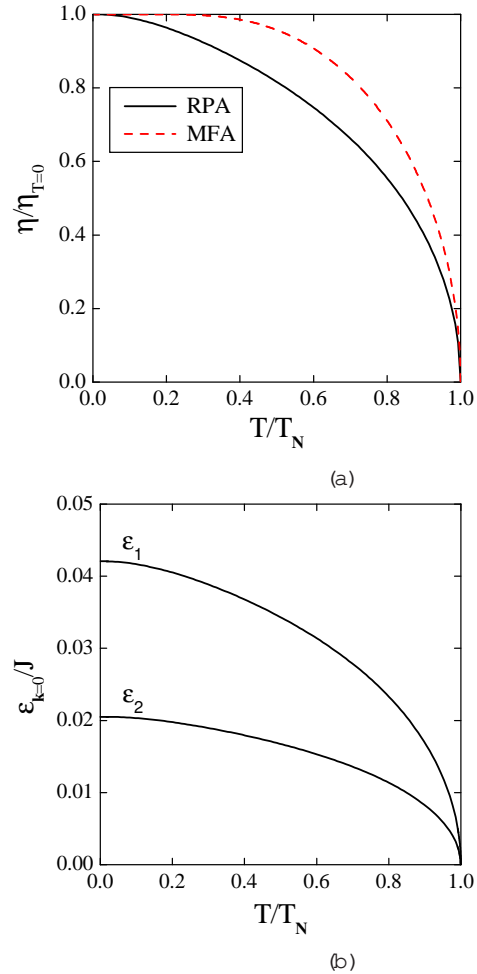


FIG. 3: (Color online) The (a) order parameter vs.  $T = T_N$  within the RPA method (black solid line) and the MFA (red dashed line), and the (b) spin-wave gaps, in units of  $J$ , in the spectrum of elementary excitations vs.  $T = T_N$  within the RPA method. In both of these figures we have used  $d/J = 0.02$ ,  $(\epsilon_1 - \epsilon_3)/J = 0.42 \cdot 10^{-3}$ ,  $\epsilon_1 + \epsilon_3 = 0$ , and  $\epsilon_2 = 0$ .

Now let us show that in contrast to the MFA approach, where  $T_N = J_2/J$  is almost independent of the anisotropy, the Neel temperature within the RPA analytical scheme is very sensitive to model parameters  $d$  and  $\epsilon_1 - \epsilon_3$ . Figure 4 shows the zero-temperature en-

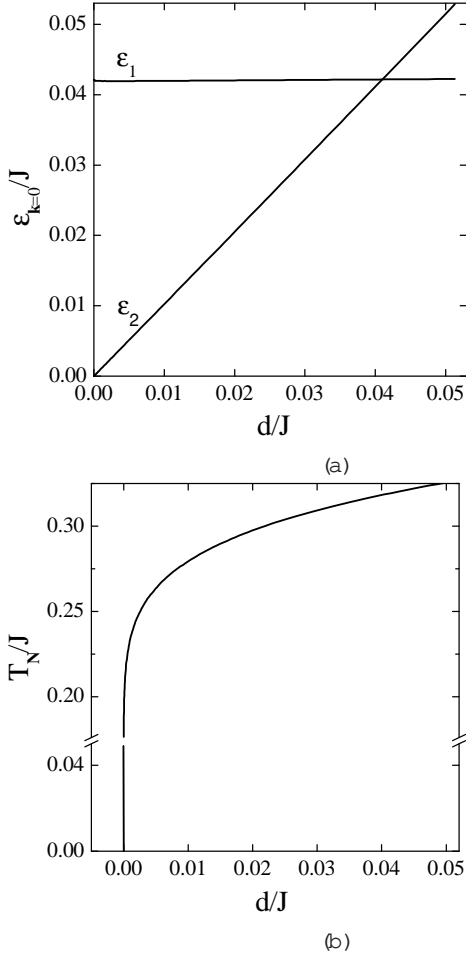


FIG. 4: The (a)  $T = 0$  energy gaps, in units of  $J$ , vs. the DM parameter  $d=J$ , as well as (b) the Neel temperature  $T_N$ , in units of  $J$ , vs  $d=J$ . In both of these figures,  $(\Gamma_1 - \Gamma_3)/J = 0.42 \times 10^{-3}$ ,  $\Gamma_1 + \Gamma_3 = 0$ , and  $\Gamma_2 = 0$ .

energy gaps and the Neel temperature as functions of the DM antisymmetric exchange interaction  $d=J$  within the RPA method. As one can see, the energy gap  $\epsilon_1$  is almost independent of the  $d=J$ , while  $\epsilon_2$  depends almost linearly on the DM interaction  $d=J$ , and in fact goes to the zero in the limit  $d=J \rightarrow 0$ . As a result, when  $d=J = 0$  the Goldstone mode appears in the spin-wave spectrum and thermal fluctuations destroy the long-range ordering for any  $T > 0$ . Consequently, the Neel temperature drops to zero in case of  $d = 0$ .

In the next two figures we present the dependencies on the model parameter  $(\Gamma_1 - \Gamma_3)/J$ . Now, the energy gap  $\epsilon_2$  is independent of the parameters of symmetric anisotropy and thus determined by the DM interaction  $d=J$  alone, while the gap  $\epsilon_1$  varies strongly with  $(\Gamma_1 - \Gamma_3)/J$ . As in the above case, in the limit of  $\Gamma_1 - \Gamma_3 \rightarrow 0$  the mode  $\epsilon_2$  in the spectrum becomes gapless and, therefore, the transition temperature to the long-range ordered state would be suppressed to zero.

One can understand the above results for the zone-

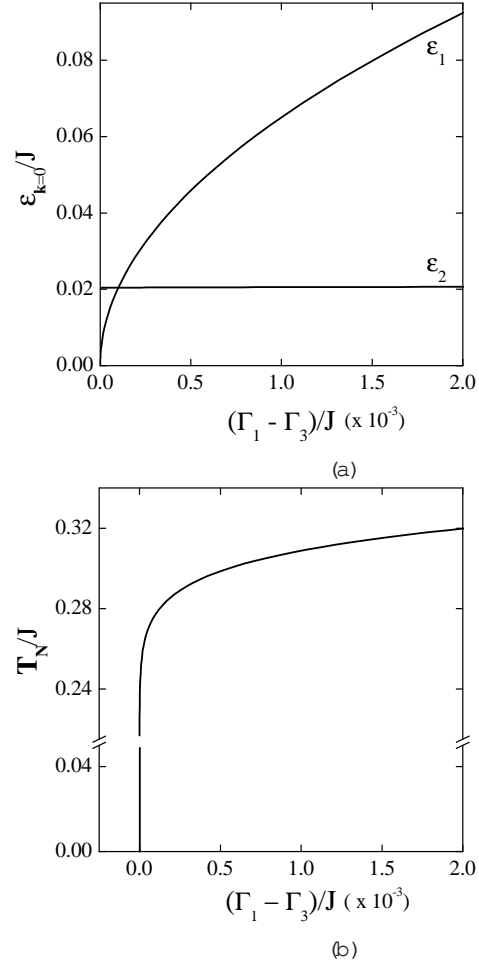


FIG. 5: The (a) energy gaps, in units of  $J$ , vs.  $(\Gamma_1 - \Gamma_3)/J$ , and (b) the Neel temperature, in units of  $J$ , as function of  $(\Gamma_1 - \Gamma_3)/J$ .

centre excitation spectrum immediately from the the expressions Eq. (104) in the limit of small anisotropy. Our numerical results, shown in the previous figures, demonstrate that these expressions are valid over a large range of parameter values.

## B. Parameters regimes

We now summarize our numerical results with regards to the dependence of various thermodynamic quantities on the material parameters appearing in the Hamiltonian.

Firstly, we find that the Neel temperature is almost independent of the  $(\Gamma_1 + \Gamma_3)/J$  within the reasonable range of the model parameters (see below). In fact, in order to argue for the independence of the thermodynamic quantities central to this study on certain material parameters that appear in the Hamiltonian, viz.  $\Gamma_2$  and  $\Gamma_1 + \Gamma_3$ , in Fig. 6 we show two representative plots for the order parameter and the susceptibility within the RPA scheme

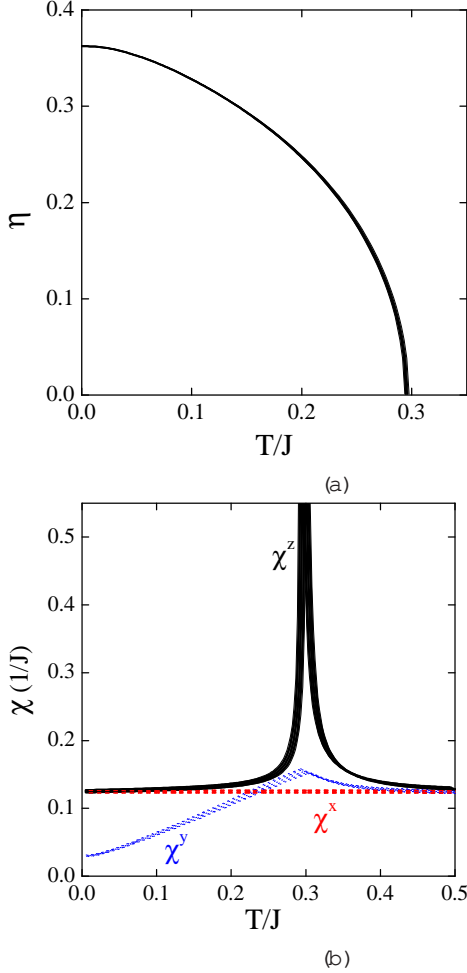


FIG. 6: (Color online) The (a) order parameter vs.  $T=J$  for the different values of  $d_2=J$  and  $(d_1+d_3)=J$ , and (b) the susceptibility, in units of  $1=J$ , vs.  $T=J$  for the different values of  $d_2$  and  $d_1+d_3$  discussed in the text. In these plots we have fixed  $d=J = 0.02$ , and  $d_2=J$  ( $d_1+d_3=J$ )  $= 0.42 \cdot 10^{-3}$ .

for the constant values of the  $d$  and  $d_2 = d_1 + d_3$  (again in units of  $J$ ). That is, in each of the plots in Fig. 6 we have simultaneously plotted ten data sets each with the different values of the  $d_2$  and  $d_1 + d_3$ , where the parameter ratio  $d_2$  has been varied from the value  $10^3$  up to the  $10^2$ , and  $d_1 + d_3$  from the value  $10^2$  to the  $10^3$  (all in units of  $J$ ). As one can see, even for such a large range of the parameters, one can hardly see the difference of the absolute values of the Neel temperature, order parameter and susceptibility.

Thus, to study the magnetic properties of the system we can use only the DM interaction  $d$  and the combination  $d_1 + d_3$  of the symmetric tensor components as two independent parameters, and so we conclude (similar to others<sup>32,33</sup>) that the system can be studied using  $d_2 = 0$  and  $d_1 + d_3 = 0$ .

In various limits, it can be shown that this result follows from the above presented analytical work. The non-diagonal term  $d_2$  of the symmetry anisotropy tensor is

involved in all expression through the combination in the  $J_4$  (Eq. (8)). For the reasonable anisotropy parameters (that is  $d < d_1 + d_3$ ) the spins are canted by a very small angle  $d_2=J$ , and as a result we can neglect the term  $d_2 \sin d_2=J$  with respect to  $d$ , and hence we can ignore the quantity  $d_2$  in all our formulae. Similarly,  $d_1 + d_3$  is involved in the formulae through the combination in the  $J_2, J_3$ , and canted angle  $\theta$ , where it appeared only as the combination  $J + \frac{1}{2}(d_1 + d_3)$ . Thus, the parameter  $d_1 + d_3$  can be ignored with respect to the superexchange interaction  $J$  (see Eq. (8)).

Therefore, one can assert that the model Hamiltonian of Eq. (1) leads to the same results as, for instance, the model described by the spin Hamiltonian

$$H = \sum_{\langle ij \rangle} [J S_i \cdot S_j + D_{ij} (S_i^z - S_j^z)]; \quad (109)$$

where we define  $d_1 = d_3$ .

### C. Susceptibility

Now let us consider the main focus of our paper, that being the behaviour of the different components of static uniform magnetic susceptibility as a function of temperature. Our results for  $\chi^x$ , for the parameters discussed in the previous subsections, are shown in Fig. 7 (recall our earlier result that the MFA and SW theories predict the same  $T$ -independent value for this quantity). The  $x$  component of susceptibility below the Neel temperature is the temperature independent and is equal to  $\chi^x = (8J)$  within the MFA (Eq. (45)), the RPA scheme (Eq. (82)), or spin-wave theory (Eq. (85)). However, above the ordering temperature, the RPA and MFA yield different results, with a weak  $T$ -dependence within the RPA, while a strong Curie-like falloff is found within the MFA.

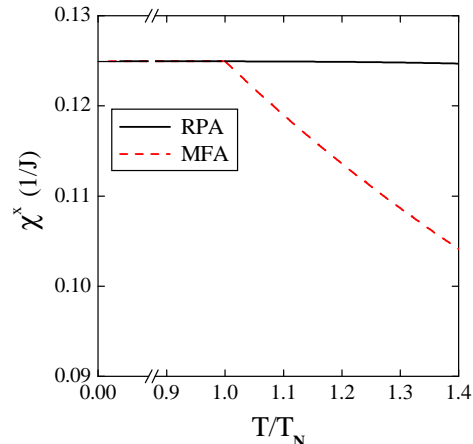


FIG. 7: (Color online) The susceptibility  $\chi^x$ , in units of  $1=J$ , within the RPA (black solid line) and MFA (red dashed line), for the parameters values  $d=J = 0.02$  and  $d_2=J = 0.42 \cdot 10^{-3}$ . Below  $T_N$  these theories both predict the same constant value that is independent of temperature.

As we will discuss in a future publication, this behaviour changes if one includes 4-spin ring exchange, or goes beyond the Tyablikov RPA decoupling scheme that we employ in this paper. This is important since the experimental data of Lavrov et al.,<sup>6</sup> shows a small nonzero slope of  $\chi^x$  vs.  $T$ . Indeed, a successful comparison with the small slope seen below  $T_N$  in experimental data<sup>6</sup> necessarily requires that we go beyond the treatment of spin-wave interactions and/or Hamiltonian that are included in this paper. We emphasize that the necessity of going beyond the Tyablikov RPA decoupling to obtain this slope is a manifestation of the presence of strong quantum fluctuations, a theme that will be repeated in our discussion in this and the next section of this paper.

Our results for the  $y$  component of the susceptibility,  $\chi^y$ , are shown in Fig. 8. These plots show that be-

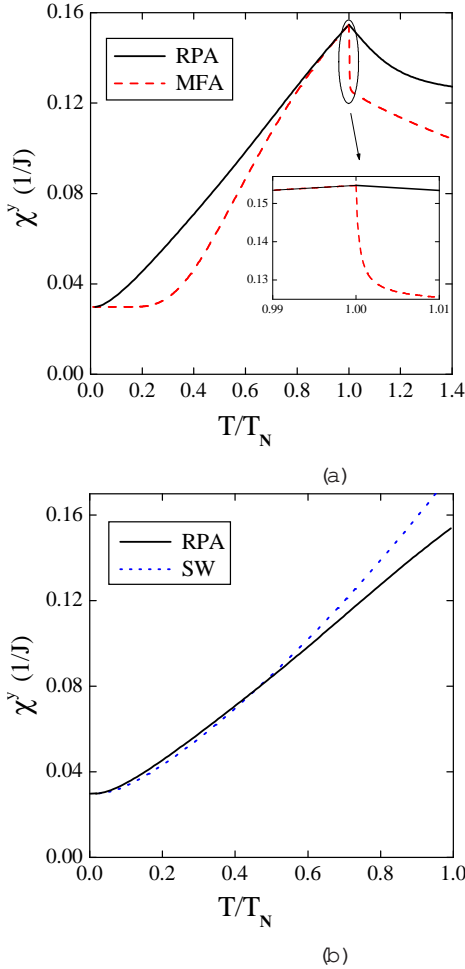


FIG. 8: (Color online) The (a) susceptibility  $\chi^y$  within the RPA (black solid line) and MFA (red dashed line), and (b) a comparison of the RPA (black solid line) and spin-wave (SW) (blue dotted line) results below  $T_N$ . As in previous figures, we are using  $d=J = 0.02$  and  $\hbar=J = 0.42 \times 10^{-3}$ .

low the ordering temperature the RPA scheme leads to the good agreement with the MFA scheme near the  $T_N$  ( $0.8T_N < T < T_N$ ), and good agreement with the SW

theory at low- $T$  (that is, for  $T < T_N/2$ ). Above the Neel temperature, the RPA and MFA theories lead to very different results. The MFA method gives an abrupt decrease of  $\chi^x$  to a value that is close to that of the purely transverse component  $\chi^x = 1/(8J)$  (see inset of this figure), while the RPA leads to a much more gradual decrease of the value of  $\chi^y$  with the temperature.

The  $z$  component of the susceptibility,  $\chi^z$ , is shown in Fig. 9. We find that at low  $T$ , as was also found for  $\chi^y$ ,

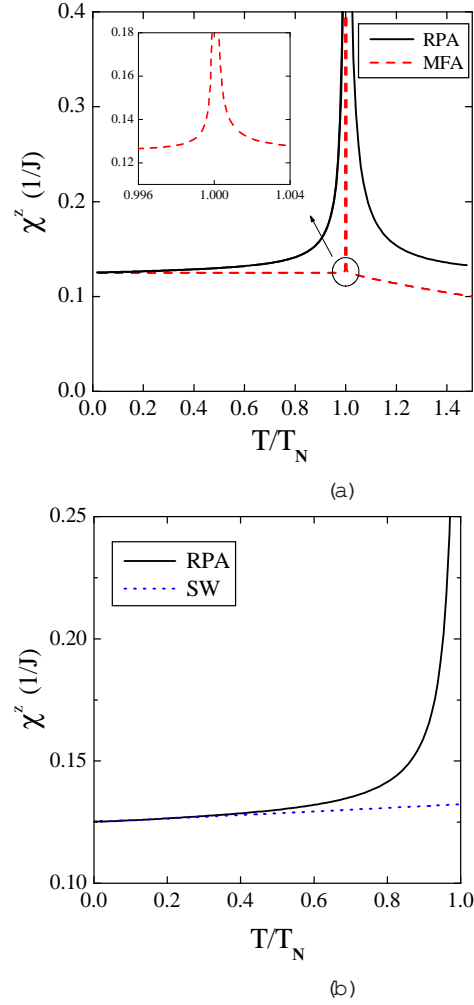


FIG. 9: (Color online) The susceptibility  $\chi^z$  within (a) the RPA (black solid line) and MFA (red dashed line), as well as (b) a comparison of  $\chi^z$  below the ordering temperature within the RPA (black solid line) and spin-wave (SW) (blue dotted line) theory. As in previous plots, we have used  $d=J = 0.02$  and  $\hbar=J = 0.42 \times 10^{-3}$ .

the RPA is in the the good agreement with spin-wave predictions. Near the transition temperature, the RPA method leads to the qualitatively different behaviour of the  $z$  component of susceptibility with respect to both the MFA and spin-wave formalisms.

The differences between the MFA vs. RPA data shown above can be understood using the following reasoning. Firstly, consider below the Neel temperature. The canted



moments which develop are confined to lie in the  $y-z$  plane; as well, they are ferromagnetically ordered in the  $z$ -direction (recall that we are studying a single  $\text{CuO}_2$  plane). Then, one can see that within the MFA the weak FM produces a divergence of the  $z$ -component of the susceptibility only in a very narrow temperature region close to the Neel point. Since the MFA does not account for near-neighbour correlations between the spins, away from the immediate vicinity of  $T_N$  the weak FM is ignored and  $\chi^z$  behaves like a  $T$ -independent transverse susceptibility (that is, transverse to the ordered AF moment). In contrast to this, the  $z$ -component of the susceptibility calculated within the RPA has a strong temperature dependence and shows that the effects of the quantum fluctuations are important in a wide region below the Neel temperature. The other component which shows some differences between the MFA and RPA below the transition is  $\chi^y$ , and for this component it is seen that since the MFA does not include the reduction of the staggered moment (which is in this direction) due to quantum fluctuations at low temperatures, linear spin-wave theory, and not the MFA, agrees with the RPA for low temperatures.

Further, above the Neel temperature the differences can be understood as follows. In a MFA (that is  $T_N^{\text{MFA}} = J$ ), both components of the susceptibility  $\chi^y$  and  $\chi^z$  are rapidly changing functions in the immediate vicinity of  $T_N$  ( $T = T_N \pm 0.005$ ), and then have the same behaviour as the  $\chi^x$  term further above the transition. This MFA behaviour is in no way similar to that found in the RPA. That is, our results are an example of the pronounced effects of short-range correlations and quantum fluctuations. The RPA scheme gives a much lower value of the Neel temperature than MFA does ( $T_N = 0.3J$ ), but in a broad  $T$  region above the Neel point strong short-range correlations exist, and the RPA includes the manner in which these fluctuations strongly modify the susceptibility. Similar reasoning explains the differences in  $\chi^x$  between the MFA and RPA.

For completeness, in Figs. 10, 11, 12 we present all components of the susceptibility together, within both the MFA and the RPA, contrasting different values of the physical parameters describing the DM interaction. To be specific, in Fig. 10 we show the situation when  $\epsilon_1 > \epsilon_2$  with the ratio  $(\epsilon_1/\epsilon_2)^2 = 4.2$  at zero temperature. As a result, we obtain that for  $T = 0$   $\chi^y < \chi^x$ ;  $\chi^z$  with the same ratio between the  $x/z$  and  $y$  components of susceptibility  $\chi^x/\chi^z = \chi^y$  4.2 (see xIV D). By increasing the magnitude of the DM parameter  $d$ , due to the strong dependence of the mode  $\epsilon_2$  of the  $d$  (see Fig. 4), we obtain the situation corresponding to  $\epsilon_2 = \epsilon_1$ . Then, as is seen in Fig. 11, both the MFA and RPA schemes result in equal values of the all components of susceptibility at low  $T$ . A further increasing of  $d$  leads to the situation  $\epsilon_2 > \epsilon_1$ , opposite to the one presented in Fig. 10. In Fig. 12 we show the susceptibility in the case of the ratio  $(\epsilon_2/\epsilon_1)^2 = 2.0$ , and at  $T = 0$  one finds  $\chi^y > \chi^x$ ;  $\chi^z$  and  $\chi^y = \chi^x/\chi^z = 2.0$  for  $T = 0$ . (We note that for other sets of  $d$ ;  $\epsilon$ , the behaviour of the components of  $\chi$  is

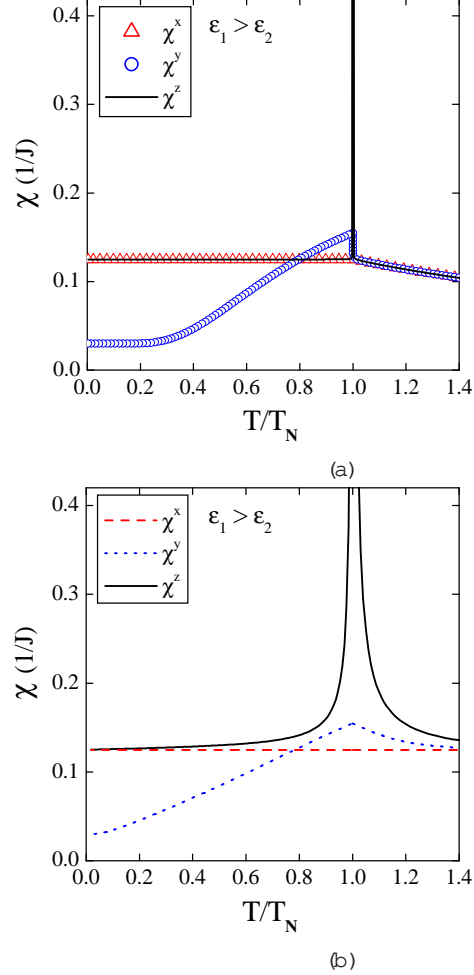


FIG. 10: (Color online) All 3 components of the susceptibility within (a) the MFA, and (b) within the RPA, for  $d = J = 0.02$  and  $\epsilon_1/\epsilon_2 = 4.2$ .

determined almost entirely by the ratio of the spin-wave gaps,  $\epsilon_1/\epsilon_2 = 4.2$ . These results agree with our analytical predictions (see section IV.)

Then, comparing the  $z$ -component of the susceptibility within the RPA (Figs. 10(b)-12(b)) we also find that increasing of the anisotropy parameter  $d$  leads to the broadening  $T$  regions where (i) the effects of the quantum fluctuations are important  $T < T_N$  and (ii) the strong short-range correlations exist  $T > T_N$ .

## VI. SUMMARY AND CONCLUSIONS/DISCUSSION

To summarize, we have presented a theoretical investigation of a single  $\text{CuO}_2$  plane of the undoped  $\text{La}_2\text{CuO}_4$  crystal in the low- $T$  orthorhombic phase. The Cu spins in the plane were modelled by the 2D spin-1/2 Heisenberg AF with spin-orbit coupling, the latter represented the antisymmetric and symmetric DM anisotropies. We have adopted the Green's function

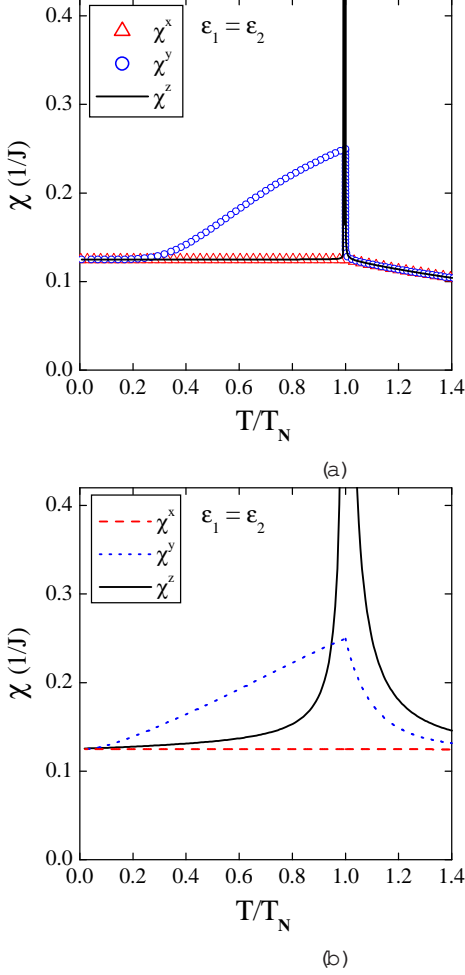


FIG. 11: (Color online) All 3 components of the susceptibility within (a) the MFA, and (b) within the RPA, for  $d=J=0.041$  and  $\epsilon_1=\epsilon_2=0.42 \times 10^{-3}$ .

method within Tyablikov's RPA decoupling scheme to calculate the magnetic susceptibility of such a model. In order to allow us to accurately model the longitudinal susceptibility within such a level of decoupling of high-order Green's functions, we have extended Liu's method<sup>17</sup> for the isotropic Heisenberg model to one that includes a weak canted FM moment in the plane.

We can emphasize several important conclusions from our results. We have found that the anisotropy introduced into the problem by the symmetric and antisymmetric DM interactions leads to important changes in the behaviour of the magnetic susceptibility near the transition point. By comparing the MFA and RPA results we conclude that the effects of quantum fluctuations and the short-range correlations are very strong in the broad temperature region of near the Neel temperature. Further, we find that since the RPA and SW results are quite different near the Neel temperature, the effects of spin-wave interactions, which are included in an approximate way in the RPA but not the SW theories, are very important in this system. This neces-

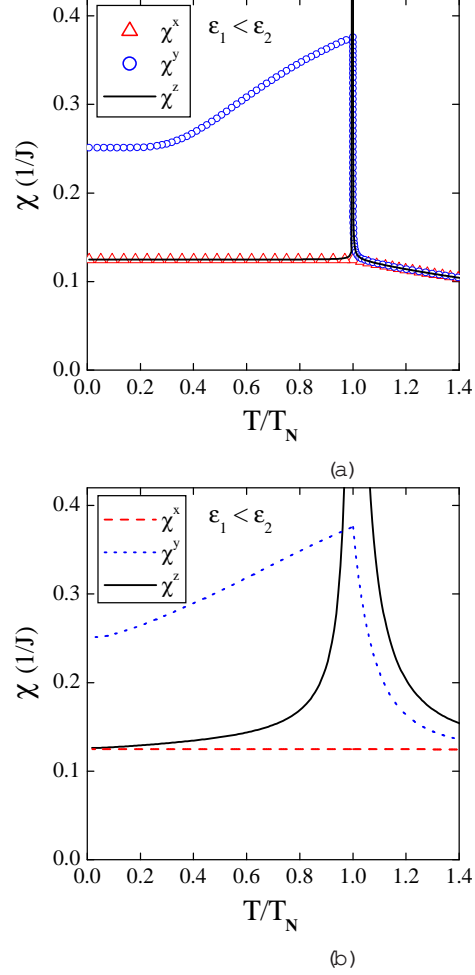


FIG. 12: (Color online) All 3 components of the susceptibility within (a) the MFA, and (b) within the RPA, for  $d=J=0.058$  and  $\epsilon_1=0.42 \times 10^{-3}$  and  $\epsilon_2=0.58 \times 10^{-3}$ .

sarily leads to the question, would more advanced decoupling schemes, namely improvements on Tyablikov's decoupling (e.g., see our Eq. (59)), or, possibly, the inclusion of nonlinear effects in the SW theory, lead to qualitatively different results?

Secondly, we have obtained that the weak ferromagnetism in the z-direction (caused by the DM interaction) leads to the essential difference between the temperature behaviours of the transverse  $\chi^x$  and  $\chi^y$  components of the susceptibility (recall that the AF moments lie in the y-z plane and are nearly aligned along the y axis). We established the correlation between the ratio of the in- and out-of-plane spin-wave modes of the excitation spectrum in the long wavelength limit ( $k=0$ ), which is fixed by the ratio between the  $d$  and  $\epsilon_1/\epsilon_3$  DM parameters, and the behaviour of  $\chi^x/\chi^y$  vs.  $T$  in the zero temperature limit. This conclusion is independent on the analytical method which we used to calculate the susceptibilities, since all methods agree in the low- $T$  regime, and could allow one to make predictions concerning the gaps in the excitation spectrum based on the data for the suscepti-

bility.

Now we comment on the comparison of our results to the experimentally observed anisotropies<sup>6</sup> that motivated this work. We can state that, in addition to the known results<sup>12,13,14</sup> that DM interaction induces the weak ferromagnetism in the LTP phase and the spin-wave gaps, this interaction is at least in part responsible for the unusual anisotropy in the magnetic susceptibility.<sup>6</sup> We can mention the most significant features observed in the experiment that are in qualitative agreement with the presented in paper theoretical results: (i) the absence of any special behaviour (anomaly) in the transverse component  $\chi^x$  across the Neel temperature; (ii) the additional increase of the  $\chi^y$  component in the ordered state and its smooth decrease in a broad temperature region in the paramagnetic state; (iii) a significant temperature dependence of the component  $\chi^z$  in the broad temperature region below and above the transition point.

Now we briefly discuss the experimental data which cannot be explained within the framework of the proposed here theory. Firstly, we have found that the observed ratio between the  $x$  and  $y$  components  $\chi^x < \chi^y$  (in the  $T = 0$  limit) takes place only if the spin-wave gap with out-of-plane mode is less than the in-plane one  $\omega_o < \omega_i$ . However, older neutron-scattering experiments<sup>5</sup> find the opposite ratio: the magnitude for the out-of-plane mode is 5 meV, for the out-of-plane mode 2.3 meV. Recent Raman work confirms one of these values.<sup>32</sup> So, other interactions which affect these gaps must be important for an accurate explanation of the susceptibility data. Secondly, our results cannot explain a  $T$ -

independent shift between  $\chi^x$ ;  $\chi^y$  and  $\chi^z$  observed in experiments (an explanation of this physics is provided in the experimental paper, namely that one must include a van Vleck contribution which shifts, in a  $T$ -independent manner, these components of the susceptibility, but we defer our inclusion of this physics until the second paper in this series of theoretical studies.

For further improvements of our theoretical modelling of the  $\text{La}_2\text{CuO}_4$  compound, it seems to be important to investigate a 3D model on a body-centered lattice with the weak AF interlayer coupling. It is also possible to extend the 2D model by considering the ring exchange, and the interaction between the next nearest neighbour sites, and we expect that some of these additional physics can be responsible for the correct ratio between the spin-wave gaps with respect to the ratio between  $\chi^x$  and  $\chi^y$ . In addition, the anisotropic Van Vleck contribution (orbital susceptibility) and gyromagnetic (Lande) factor need to be taken into account. We will present a detailed comparison to these experiments when these other interactions are included in future publications.

#### Acknowledgments

We wish to thank Yoichi Ando, Alexander Lavrov and David Johnston for helpful discussions. One of us (R.J.G.) thanks the Aspen Center for Physics, where part of this work was completed. This work was partially supported by the NSERC of Canada and NATO.

Electronic address: tkir@physics.queensu.ca

- <sup>1</sup> A.J.M. Illis, H.M. Onien, and D.P. Ines. *Phys. Rev. B*, 42:167, 1990.
- <sup>2</sup> E.M. Anousakis. *Rev. Mod. Phys.*, 63:1, 1991.
- <sup>3</sup> T. Thio, T.R. Thurston, N.W. Preyer, P.J. Picon, M.A. Kastner, H.P. Jensen, D.R. Gabbe, C.Y. Chen, R.J. Birgeneau, and A. Aharony. *Phys. Rev. B*, 38:905, 1988.
- <sup>4</sup> M.A. Kastner, R.J. Birgeneau, T.R. Thurston, P.J. Picon, H.P. Jensen, D.R. Gabbe, M. Sato, K. Fukuda, S. Shamoto, Y. Endoh, K. Yamada, and G. Shirane. *Phys. Rev. B*, 38:6638, 1988.
- <sup>5</sup> B. Keimer, R.J. Birgeneau, A. Cassanho, Y. Endoh, M. Greven, M.A. Kastner, and G. Shirane. *Z. Phys. B*, 91:373, 1993.
- <sup>6</sup> A.N. Lavrov, Y. Ando, S. Komiyama, and I. Tsukada. *Phys. Rev. Lett.*, 87:0170071, 2001.
- <sup>7</sup> I.D. Zialoshinski. *J. Phys. Chem. Solids*, 4:241, 1958.
- <sup>8</sup> T.M. Oriya. *Phys. Rev.*, 120:91, 1960.
- <sup>9</sup> J. Stain. *Phys. Rev. B*, 53:785, 1996.
- <sup>10</sup> In this notation the  $c$  axis points perpendicular to the  $\text{CuO}_2$  plane.
- <sup>11</sup> T. Thio and A. Aharony. *Phys. Rev. Lett.*, 73:894, 1994.
- <sup>12</sup> D. Coey, T.M. Rice, and F.C. Zhang. *Phys. Rev. B*, 44:112, 1991.
- <sup>13</sup> L. Shekhtman, O. Ebtin-Wohlman, and A. Aharony. *Phys. Rev. Lett.*, 71:468, 1993.

- <sup>14</sup> W. Koshibae, Y. Ohta, and S. Maekawa. *Phys. Rev. B*, 50:3767, 1994.
- <sup>15</sup> J. Stain, O. Ebtin-Wohlman, and A. Aharony. *Phys. Rev. B*, 53:775, 1996.
- <sup>16</sup> S.V. Tyablikov. *Ukrain. Mat. Zh.*, 11:287, 1959.
- <sup>17</sup> K.H. Lee and S.H. Liu. *Phys. Rev.*, 159:390, 1967.
- <sup>18</sup> D.P. Arovas and A. Auerbach. *Phys. Rev. B*, 38:316, 1988.
- <sup>19</sup> S. Sarker, C. Jayaprakash, H.R. Krishnamurthy, and M.M. Ma. *Phys. Rev. B*, 40:5028, 1989.
- <sup>20</sup> T.N. de Silva, M.M. Ma, and F.C. Zhang. *Phys. Rev. B*, 66:104417, 2002.
- <sup>21</sup> M. Takahashi. *Phys. Rev. B*, 40:2494, 1989.
- <sup>22</sup> V.Yu. Izkhin, A.A. Katanin, and M.I. Katsnelson. *Phys. Rev. B*, 60:1082, 1999.
- <sup>23</sup> I. A. Aek and J.B. Marston. *Phys. Rev. B*, 37:3774, 1988.
- <sup>24</sup> A. Shern and M. Schreiber. *Phys. Rev. B*, 63:214421, 2001.
- <sup>25</sup> Yu.A. Izyumov, N.I. Chaschin, and V.Yu. Yushankhai. *Phys. Rev. B*, 65:214425, 2002.
- <sup>26</sup> S. Chakravarty, B.I. Halperin, and D.R. Nelson. *Phys. Rev. B*, 39:2344, 1989.
- <sup>27</sup> David C. Johnston. *Handbook of Magnetic Materials*, 1996.
- <sup>28</sup> N.E. Bonesteel. *Phys. Rev. B*, 47:11302, 1993.
- <sup>29</sup> D. Coey, K.S. Bedell, and S.A. Trugman. *Phys. Rev. B*, 42:6509, 1990.
- <sup>30</sup> D. Mermin and X. Wagner. *Phys. Rev. Lett.*, 17:1133, 1966.

<sup>31</sup> S.H. Liu. Phys. Rev., 142:267, 1967.

<sup>32</sup> A. Gozar, B.S. Dennis, G. Blumberg, S. Komiyama, and Y. Ando. Phys. Rev. Lett., 93:027001, 2004.

<sup>33</sup> C.J. Peters, R.J. Birgeneau, M.A. Kastner, H. Yoshizawa,

Y. Endoh, J. Tranquada, G. Shirane, Y. Hidaka, M. Oda, M. Suzuki, and T. Murakami. Phys. Rev. B, 37:9761, 1988.

